Article type : Original Article

Title: Nutrient loading effects on fish habitat quality: Trade-offs between enhanced production and hypoxia in Lake Erie, North America

Authors: L. Zoe Almeida [1,2,*], Timothy M. Sesterhenn[2,3], Daniel K. Rucinski[4], Tomas O. Höök[2,5]

[1] Ecological Sciences and Engineering Interdisciplinary Graduate Program, Purdue University, West Lafayette, IN, U.S.A.

[2] Forestry and Natural Resources Department, Purdue University, West Lafayette, IN, U.S.A.

[3] Department of Natural and Mathematical Sciences, Morningside University, Sioux City, IA, U.S.A.

[4] LimnoTech, Ann Arbor, MI, U.S.A.

[5] Illinois-Indiana Sea Grant College Program, Purdue University, West Lafayette, IN, U.S.A.

Correspondence: L. Zoe Almeida, Hatfield Marine Science Scenter, 2030 SE Marine Science Drive, Newport, OR 97365, U.S.A. E-mail: almeidle@oregonstate.edu

Running Head: Effects of nutrients on fish habitat quality

Keywords: eutrophication, climate change, growth rate potential model, Lake Erie, bioenergetics

Primary Research Article

Summary

1. Across diverse systems, nutrient loading from anthropogenic sources into aquatic systems has increased over the past century. Such nutrient inputs may enhance system productivity and thereby increase resource availability but may also lead to undesirable conditions such as hypoxic zones.
2. We examined the habitat quality trade-offs associated with increases in phosphorus in a model system (Lake Erie, North America) with a history of anthropogenic nutrient loading. Using a water quality model and a bioenergetics growth rate potential (GRP) model with fine vertical and temporal resolution, we assessed how the quality of habitat for multiple species of adult and juvenile fish changed across a range of phosphorus loading scenarios and across 19 different meteorological years.
3. Increases in phosphorus loading increased invertebrate prey biomass, but also increased the duration and extent of the mid-summer hypoxic zone. In general, phosphorus loading caused overall habitat quality to decline and only increased peak habitat quality (i.e., spatio-temporal locations where temperature and prey abundance were already above average), but responses were species- and life-stage specific.
4. One challenge in ascertaining the effects of nutrient loading on fish habitat quality is separating the negative effects of hypoxia from the potential positive effects of increased prey densities. Through various model scenarios, we evaluated the individual effects of hypoxia and increased prey availability on fish habitat quality, demonstrating their potentially counter-balancing effects. That is, the negative effects of low oxygen on fish habitat quality appear more severe if the prospect that increased hypoxia is accompanied by altered prey densities is not accounted for.
5. Despite modeled responses to altered phosphorus loads, habitat quality responded more strongly to variation in annual meteorological conditions. Annual meteorological conditions such as temperature, vertical mixing, and timing of phosphorus loading had a greater effect on habitat quality for all species and life-stages than changes in annual amount of phosphorus loading. This limited effect of changes in phosphorus loading on habitat quality likely partially reflects our focus on short-term (1-year) changes in

loading. Thus, nutrient abatement programs may not lead to obvious, rapid positive habitat quality responses, as short-term meteorological effects may overwhelm effects related to nutrient reduction and changes in prey densities may partially offset the benefits of decreased hypoxic conditions.

Introduction

Globally, increases in nutrient loading from anthropogenic sources have led to an expansion of hypoxic zones, areas with depleted oxygen typically defined as dissolved oxygen ≤ 2.0 mg · L^{-1} (Diaz & Rosenberg, 2008; Altieri & Diaz, 2019). While hypoxia develops due to natural processes in many bodies of water, the addition of nutrients from human activities can exacerbate this phenomenon by increasing system production and ultimately contributing to enhanced oxygen depletion through decomposition. In systems that experience seasonal, vertical stratification, zones of bottom water hypoxia can persist for months and cover huge areas (e.g., April – September, 14,000 km^2, northern Gulf of Mexico, Altieri & Diaz, 2019). Increased nutrient loading from rising human populations and global climate change are likely to expand the spatial extent and annual duration of bottom water hypoxic zones and cause new zones to be formed in freshwater, estuarine, and coastal marine systems (Diaz, 2001; Diaz & Rosenberg, 2008; Zhang *et al.*, 2010). Importantly, anthropogenic nutrients can also positively affect prey production (Caddy, 2000; Adamack, Rose & Cerco, 2017; Rose *et al.*, 2018). Thus, consideration of both potential positive (i.e., increased production and prey densities) and negative (e.g., reduced survival and growth due to low oxygen levels) effects will be important for elucidating population and community responses to enhanced nutrient loads.

The excess nutrients that contribute to hypoxia alter aquatic ecosystems through myriad pathways. Many studies on nutrient loading have focused on the negative effects of increased nutrient loading on fish production (e.g., Pihl, Baden & Diaz, 1991; Howell & Simpson, 1994; Roberts *et al.*, 2009; Arend *et al.*, 2011; but see Rose *et al.*, 2019). High nutrient concentrations may favor inedible forms of phytoplankton (e.g., cyanobacteria, see Paerl & Fulton, 2006), negatively affect water clarity and foraging environments (Kirk, 1977), and enhance hypoxic conditions causing direct mortality by asphyxiation or indirect changes in fish behavior and growth (Breitburg, 2002; Pollock, Clarke & Dubé, 2007; Hrycik, Almeida & Höök, 2017). However, increases in nutrients may also increase total biomass of phytoplankton, zooplankton, and benthic invertebrates, potentially providing more food for fish (Smith *et al.*, 1981; Elmgren,

1989; Blumenshine *et al.*, 1997; Rose *et al.*, 2018). While past studies have evaluated the potential effects of hypoxia on fish growth (e.g., Eby *et al.*, 2005; Almeida *et al.*, 2017), horizontal and vertical distribution (e.g., Ludsin *et al.*, 2009; Kraus *et al.*, 2015), trophic interactions (e.g., Pihl, 1994; Shoji *et al.*, 2005; Glaspie *et al.*, 2019), recruitment (Hughes *et al.*, 2015), and community composition (e.g., Howell & Simpson, 1994; Ludsin *et al.*, 2001), most have only considered effects of hypoxia and ignored the potential benefits of coincident prey increases (however, see Adamack, Rose & Cerco, 2017; Rose *et al.*, 2018).

The effect of increased nutrient loading on fish production may be species-, life-stage-, and system-specific, depending on species' and life-stage's environmental tolerances and existing system productivity levels. Species- and life-stage-specific effects of nutrient loading and subsequent hypoxia are likely regulated by the vertical structure of aquatic systems and corresponding species and life-stage distributions. Species and life-stages reliant on habitat within a hypoxic zone may decrease in abundance (e.g., Pihl, Baden & Diaz, 1991; Petersen & Pihl, 1995; Eby *et al.*, 2005; Stone *et al.*, 2020); but, fish production in areas vertically or horizontally adjacent to hypoxic areas may increase (Caddy, 1993, 2000; Rose *et al.*, 2019). And system-specific responses to increased nutrient loading may depend on physical characteristics of waterbodies (e.g., circulation, bathymetry, and flushing in semi-enclosed seas, Silva & Vargas, 2014; Avramidis *et al.*, 2015) and their current nutrient status (e.g., oligotrophic versus meso- or eutrophic systems, Caddy, 1993; Paerl & Fulton, 2006).

Temporal dynamics across various scales may affect the way in which nutrient loading influences fish habitat quality and production. Among years, meteorological conditions can contribute to variation in the size, duration, and magnitude of hypoxic zones (Del Giudice *et al.*, 2018; Altieri & Diaz, 2019). Seasonally, hypoxia has species- and life-stage-specific effects on growth, reproduction, and survival, (e.g., Arend *et al.*, 2011). Within a day, fish and zooplankton diel vertical migration (DVM) can be disrupted by hypoxia (Baldwin, Beauchamp & Gubala, 2002; Ludsin *et al.*, 2009; Vanderploeg *et al.*, 2009), potentially providing new refuges for prey (Ludsin *et al.*, 2009) or increasing overlap between predators and prey (Vanderploeg *et al.*, 2009; Brandt *et al.*, 2011). Examining the effects of nutrient loading annually, seasonally, and sub-daily will provide a more holistic understanding of how altered nutrient loadings potentially affect fish habitat quality.

In this study, we examined the effects of nutrient loading (i.e., phosphorus) on fish habitat quality within the central basin of Lake Erie, North America as a model system. Lake Erie supports large recreational and commercial fisheries (3,100,000+ fish caught recreationally, 1,900,000+ kg fish harvested commercially in just Ohio waters during 2019; Ohio DOW, 2020) while its lakewide hypoxic zone approaches the size of the Gulf of Mexico hypoxic zone (e.g., Lake Erie hypoxic zone 20-7,900 km^2 during 2000-2014, Bocaniov & Scavia, 2016). Like other systems and coastal areas with seasonal hypoxia, Lake Erie has experienced decades of anthropogenic nutrient loading contributing to variation in the size of the central basin's annual hypoxic zone (Burns *et al.*, 2005; Scavia *et al.*, 2014; Del Giudice *et al.*, 2018) and concomitant fluctuations in the abundance of hypoxia-intolerant and tolerant fish species (Ludsin *et al.*, 2001). While both nitrogen and phosphorus likely contribute to the algal blooms that create seasonal hypoxia within Lake Erie's central basin, phosphorus is the primary limiting nutrient (Del Giudice *et al.*, 2021) and the focus of nutrient reduction targets (Scavia, DePinto & Bertani, 2016). Increases in the size of the summer hypoxic zone that began in the mid-1990s appear to be related to warmer temperatures extending the period of stratification in the summer and greater frequency of storm events increasing nutrient runoff, particularly of biologically available, reactive forms of phosphorus, from the surrounding watershed in the spring (Michalak *et al.*, 2013; Scavia *et al.*, 2014). Although previous studies have examined the effect of hypoxia on Lake Erie fish habitat quality (Arend *et al.*, 2011; Brandt *et al.*, 2011; Scavia *et al.*, 2014; Stone *et al.*, 2020), none to our knowledge have considered the potential tradeoffs between prey availability and hypoxia caused by fluctuations in nutrient inputs, nor have they considered the various temporal scales over which these tradeoffs could occur. Future climatic changes will likely continue to amplify nutrient loading and hypoxia in aquatic systems such as Lake Erie (Altieri & Diaz, 2019), and thus, improved understanding of the effects of nutrient loading and hypoxia on fish habitat quality is relevant to elucidate the effects of both past and potential future conditions throughout the globe.

In general, our goals were to incorporate potential positive and negative effects of phosphorus loading in calculating an index of habitat quality via growth rate potential (GRP) modeling (Brandt, Mason & Patrick, 1992) at annual, seasonal, and sub-daily timescales for six species-life-stage combinations of fishes that span a range of feeding and habitat guilds. Specifically, our objective was to evaluate the trade-off between forage base production and

hypoxia for each species and life-stage by developing phosphorus response curves, incorporating a breadth of meteorological conditions. Response curves demonstrate how a species' response may change at differing levels of a focal variable (in this case, phosphorus loading levels), and have previously been used to determine thresholds at which nutrient loading begins to detrimentally affect aquatic ecosystems (Lyche Solheim *et al.*, 2008; Trolle, Skovgaard & Jeppesen, 2008; Rucinski *et al.*, 2014; Kuiper *et al.*, 2015). Past applications of response curves to nutrient loading generally have not considered fish or upper food web responses (but see Scavia *et al.*, 2014; Kuiper *et al.*, 2015), and many applications have not thoroughly considered inter-annual effects, despite the potential for timing of nutrient loading and annual physical conditions to strongly mediate system effects of nutrient loading (e.g., Deutsch *et al.*, 2011; Hughes *et al.*, 2015; Del Giudice *et al.*, 2018). We hypothesized that 1) habitat quality of all species and life-stages would increase with increases in phosphorus at low levels (10 – 30% of average 1987-2005 levels); however, 2) at higher phosphorus levels (above 100% of average 1987-2005 levels), increasing loads would lead to decreased habitat quality depending on habitat preferences (Appendix S1, Table S1). Specifically, we expected the habitat quality of species and life-stages that feed pelagically and/or are more tolerant of warmer temperatures to benefit from increased nutrient input over a greater range of phosphorus loading.

Methods

Habitat Models

We evaluated how phosphorus loading may affect habitat quality for four fish species inhabiting the central basin of Lake Erie, using a vertical, one-dimensional (1D) water quality model (Rucinski *et al.*, 2014) to provide input habitat conditions for a bioenergetics growth rate potential (GRP) model. As developed by Brandt, Mason & Patrick (1992), GRP is intended as an index of habitat quality and not a direct predictor of growth or distribution. These types of habitat quality models have been used extensively (Brandt, 1993; Budy, Baker & Dahle, 2011; Jensen *et al.*, 2011; May *et al.*, 2012), including in Lake Erie (Arend *et al.*, 2011; Brandt *et al.*, 2011; Stone *et al.*, 2020), to consider how physical, chemical, and biological variables in a defined area of habitat may affect a hypothetical fish's energy budget, that is, a species-specific index of habitat quality.

Our GRP model builds from a coarser Lake Erie hypoxia GRP model presented by Arend *et al*. (2011) by incorporating a finer temporal resolution (e.g., 10-minute time steps), light and prey dynamics (e.g., vertical distribution updated every 10-minutes), and incremental changes in phosphorus loading (i.e., loading factors) to examine the less-studied trade-off between increased prey availability and hypoxia on fish habitat quality. We modeled habitat quality at fine vertical (0.5 m) and temporal (10 min) resolution for adults of four economically and ecologically important fish species (i.e., yellow perch, *Perca flavescens*, rainbow smelt, *Osmerus mordax*, emerald shiner, *Notropis atherinoides*, and round goby, *Neogobius melanostomus*) and young-of-year life-stages for two species (yellow perch and rainbow smelt). These modeled species and life stages encompass a range of hypoxia sensitivity, warm-water and cool-water preferences, pelagic and benthic feeders, and native and invasive species (Appendix S1, Table S1).

Model Description

The GRP model quantifies how spatio-temporal overlap of environmental conditions (e.g., temperature, dissolved oxygen, light, and pelagic and benthic invertebrate prey densities) in a 24 m 1D column of water (48 layers, each 0.5 m deep) in the central basin of Lake Erie potentially affect habitat quality for each of the six representative fish species and life-stages (Fig. 1, 2). For each application (year) of the model, simulations began on April 15 and ended on December 29, thereby encompassing the growing season for most fish species in Lake Erie and the time periods before, during, and after hypoxia occurs. Each day, the model integrated environmental conditions to quantify GRP in every 0.5 m cell at 10 min time steps (Fig. 1, 2). The model was reset at the beginning of each year, and each year, termed 'meteorological year,' is unique in its temperature, vertical mixing, timing, and magnitude of phosphorus loading, and surface lighting. All GRP modeling was performed using IDL® version 8.7.2 (Harris Geospatial Solutions Inc., 2019) and all line graphs were created with SigmaPlot version 14.5 (Systat Software Inc., 2017) or in R (R Core Team, 2021) with packages "ggplot2" (Wickham, 2016) "ggpubr" (Kassambara, 2020), and "cowplot" (Wilke, 2020).

The input data for the GRP model were obtained from 1D linked thermal and eutrophication models (Rucinski *et al.*, 2014). These inputs included daily depth-specific water temperature (°C), daily depth-specific oxygen concentration ($mg \cdot L^{-1}$), 10 min intervals of light intensity ($ly \cdot day^{-1}$) with daily depth-specific extinction factors, daily total water column

zooplankton biomass (mg · L^{-1}), and daily carbon settling to the benthos (g · m^{-2}) (Fig. 1). Full documentation of the linked thermal and eutrophication models is presented in Rucinski *et al*. (2014).

Spatiotemporal densities of zooplankton and chironomids were included as potential prey when indexing GRP. Prior to incorporating zooplankton as a component of GRP quantification, zooplankton biomass was divided into small (0.2 mm), medium (0.83 mm), and large (1.25 mm) size classes based on proportional abundances of taxa within each size class observed in the field (0.423, 0.199, and 0.378, respectively, Makarewicz, Lewis & Bertram, 1989). To capture diurnal changes in vertical distributions, total zooplankton densities were re-distributed among habitat cells at each 10 min time step based on temperature, light, and oxygen preferences of zooplankton taxa, calibrated to be within the range of observed densities in the epi- and metalimnion at specific times throughout the day at sites in Lake Erie during 2005 (see Figures 6-8 in Vanderploeg *et al.*, 2009). Chironomid (benthic prey) biomass in the bottom 1.5 m was updated daily based on modeled temperature and settling of carbon to the benthic layer. Chironomid biomass was modeled as unaffected by dissolved oxygen since previous studies have indicated that chrinomid density and body size did not differ between hypoxic and normoxic locations (Goto *et al.*, 2017). For more details on modeled prey densities and distributions, see Appendix S1 "Prey abundance and distribution" (pages 4-10).

Input data were used to calculate GRP in each 0.5 m cell during every 10 min time step using existing species-specific bioenergetics parameters (Kitchell, Stewart & Weininger, 1977; Fig. 1; Table S1). Consumption potential was modeled using a foraging sub-model based on a multi-species type-2 functional response (*sensu* Rose *et al.*, 1999) with encounter rate and proportional capture efficiency integrated. Encounter rate was affected by the size of the species and life-stage, the size of the prey item, temperature, light, and prey densities, incorporating volume of water searched, swimming speed, and reactive area equations defined in experimental studies (e.g., Hergenrader & Hasler, 1967; Breck & Gitter, 1983; Blaxter, 1986; Breck, 1993). Proportional capture efficiency accounted for predator prey preference (Rose *et al.*, 1996; Graeb *et al.*, 2004; Fulford *et al.*, 2006; Pothoven *et al.*, 2009) and prey density. A species- and life-stage-specific dissolved oxygen function reduced consumption potential when dissolved oxygen concentrations were below a critical threshold. For more information on bioenergetics and

foraging model components see Appendix S1 "Growth rate potential calculation" and "Foraging sub-model calculation" (pages 10-20).

Model Analyses

We applied water quality and GRP models for three analyses. First, to assess past habitat quality, we modeled GRP for each species and life-stage using the phosphorus loading of each respective meteorological year 1987-2005 (analyses referred to as "Hindcasts"; Rucinski *et al.*, 2014). Second, we used the models to develop phosphorus loading response curves. That is, we applied models with incremental changes in phosphorus loads and evaluated GRP responses (termed "Response Curves"). Third, we used a diagnostic approach, adjusting the occurrence of hypoxia or prey consumption potential within the GRP model to develop response curves to separate the positive effect of phosphorus on prey abundance versus the negative effect of increased hypoxia (termed "Diagnostic Application"). For all model applications, we examined GRP responses to physical and biological variables at sub-daily, daily, and seasonal scales, and we assessed annual patterns of environmental conditions and three metrics of habitat quality for all fish species and life-stages: 1) an annual index of beneficial habitat quality (percentage of positive GRP cells; Brandt *et al.*, 2011); 2) an annual index of average habitat quality (average GRP); and 3) an annual index of the best habitat (GRP-99%). The percentage of positive GRP cells is the percentage of habitat cells that are positive, where "cells" are 10 min intervals of each 0.5 m depth layer. Average GRP is the average of the GRP from every time step and depth cell throughout a year. Note that, due to the similarity in results between percentage of positive GRP cells and average GRP, average GRP results are presented in Appendix S1 ("Supplemental results on average GRP response to increases in phosphorus" pages 29-30). GRP-99% is the average of the highest 1% of GRP values across all (1,790,210) cells in a simulated year. The goal of the GRP-99% metric was to allow for a targeted analysis of the "best" habitat quality, a contrast to the overall average GRP which could include areas of habitat somewhat irrelevant to fish performance given that fish may avoid areas of poor habitat. Additionally, GRP-99% may be particularly informative, as spatial and temporal peaks in habitat quality may contribute disproportionately to annual performance of individuals (e.g., Forsman & Lindell, 1991). To ensure that examining 1% of cells incorporated habitat representative of the water column, seasons, and times of day, we examined the location of habitat cells used to calculate GRP-99%

for each species and year and compared results to a GRP-95% metric that used the top 5% of GRP values across habitat cells (Appendix S1 "Ensuring GRP-99% represents a variety of spatiotemporal habitat cells" pages 25-29).

To create a phosphorus loading response curve that accounted for annual variability in temperature, vertical mixing, timing of phosphorus loads, and light (Response Curves), we modeled GRP for each meteorological year with 19 phosphorus loads (termed "loading factors"): 0.1 increments from 0.1 to 1.9 times the annual phosphorus load during 1997, an approximately average loading year over the time series (total 1997 phorphorus load = 11,119 MT, Fig. 3, Table 1; Rucinski *et al.*, 2014). Note that while the total annual phosphorus load was scaled to 1997, all other meteorological variables, including timing of phosphorus loading, were specific to the meteorological year modeled. With the resulting 361 simulations, we examined how incremental changes in phosphorus loading affect hypoxia, prey production, and GRP for each species and life-stage. To evaluate how species- and life-stage specific annual GRP summary indices (i.e., percentage of positive GRP cells, average GRP, and GRP-99%) were affected by altered phosphorous loading, we quantified mean relative percentage change of index values (relative to mean index value at baseline 1.0 × phosphorus loading).

To diagnostically separate the influence of phosphorus loading on habitat quality acting through either hypoxia or prey availability (Diagnostic Application), we repeated phosphorus response curve analyses while fixing either oxygen concentrations or daily prey availability. Specifically, to remove the negative influence of hypoxia and focus on the positive influence of increasing prey, we applied the GRP model across loading intervals with a constant concentration of 10 mg $O_2 \cdot L^{-1}$ in every depth cell throughout the year. At this high oxygen level, there is no negative effect of oxygen on prey consumption in the foraging model. Prey abundances were still affected by increases in phosphorus, but zooplankton vertical distributions were only influenced by light and temperature since oxygen was uniform throughout the entire water column. Thus, the habitat quality response to phosphorus in the diagnostic application with no change in oxygen primarily reflected phosphorus-induced changes in prey biomass. In contrast, to remove the positive effect of increased prey biomass and focus on the negative effect of hypoxia, we applied the GRP model across loading intervals allowing for potential decreases in oxygen concentrations while prey biomasses were not allowed to differ from the biomasses produced at 1.0 × phosphorus loading for each meteorological year (Appendix S1 "Supplemental

results on model assessments of DO and prey" page 30-37). Thus, prey biomasses differed among meteorological years, fluctuated seasonally, and redistributed in response to temperature, light, and dissolved oxygen (including hypoxia), but daily total zooplankton and chironomid biomasses (integrated across the water column) did not increase or decrease due to changes in annual phosphorus loading. Therefore, habitat quality responses to phosphorus only reflected changes in oxygen concentrations.

Results

Hindcasts

Our model integrated physical and biological factors on a 10 min time step to produce retrospective depictions of habitat quality. As an example, consider adult yellow perch GRP during 2002, a moderate meteorological year (e.g., temperatures were not unusually cool or warm; Fig. 2; Appendix S1, Fig. S5-6). On a representative day after stratification and hypoxia had developed (e.g., September 15, 2002), light gradually increased at the surface of the water throughout the day, reaching its maximum intensity and deepest depth at midday (Fig. S5). Zooplankton biomass distribution responded to these changes in light, along with vertical gradients of temperature and dissolved oxygen, with an apparent diel vertical migration and avoidance of hypoxia. In response to the modeled environmental conditions, adult yellow perch GRP was relatively high in time and space when light was strong enough to allow for efficient visual foraging and where zooplankton was most dense. Throughout 2002, seasonal and diurnal changes in physical and biological conditions (Fig. S6) were reflected in habitat quality responses for each species and life-stage (Appendix S1, Fig. S7). For adult yellow perch, these spatio-temporally finely resolved analyses resulted in 12.8 % of cells (229,162 of 1,790,210) displaying positive GRP, an average GRP of -4.68×10^{-3} g · g^{-1} · d^{-1}, and a GRP-99% (highest 1% of values) of 0.007 g · g^{-1} · d^{-1} occurring in the middle of the water column during June – July (Fig. S7, Fig. 3).

Across multiple years, physical input variables differed and appeared to drive inter-annual differences in extent and magnitude of hypoxia, as well as biological responses (Fig. 3). Total phosphorus (TP) loading to the central basin of Lake Erie and average annual temperature fluctuated across years (Fig. 3a). These two factors contributed to 1) the modeled spatial and temporal extent of hypoxic conditions (Table 2, Fig. 3b) and 2) the mean modeled densities of

zooplankton and chironomid prey (Table 2, Fig. 3c). Zooplankton biomass was highly correlated (|Spearman's ρ| > ~ 0.7) with all metrics of habitat quality for all species and life stages other than adult round goby (Table 2). Correlations among other environmental variables and habitat quality metrics differed depending on species and habitat quality metric. For more plankton-oriented species and life-stage groups (i.e., all but adult round goby), temperature was negatively correlated with metrics of peak habitat quality (GRP-99%, Table 2). However, adult round goby annual habitat quality indices were positively associated with annual temperature, with a significant relationship between temperature and round goby GRP-99%. Mean annual habitat quality was variable across years for all species and life stages, with a large decrease in annual habitat quality metrics for most species and life-stages (excluding adult RG) during 1998 and 1999 (Fig. 3d-f). This decrease (as well as a more modest decrease in 1990) appeared to be due to high temperatures and lower zooplankton biomass during those years. Warmer temperatures may have negatively affected zooplankton in these years (Table 2).

Phosphorus Loading-Habitat Quality Response Curves

Our response curve analyses demonstrated the importance of meteorological conditions (e.g., thermal conditions, vertical mixing, and timing of phosphorus loading) on habitat quality. In fact, differences in meteorological year had a stronger influence on annual GRP than a 19 × range in annual phosphorus loading, thereby demonstrating the importance of developing response curves using multiple meteorological years. Despite this variation, overall habitat quality clearly responded to phosphorus loading.

An increase in the loading factor from × 0.1 to × 1.9 resulted in an increase of hypoxia extent and magnitude and a modest increase in prey (Fig. 4). The percentage of vertical habitat cells with dissolved oxygen less than 2.0 mg · L^{-1} was zero at low loading factors but expanded with even small increases in loading (Fig. 4a). Greater phosphorus loads led to modest increases in zooplankton and chironomid biomass primarily during the times of the year when these groups are typically abundant (i.e., June for zooplankton and September to mid-October for chironomids; Fig. S8), which was reflected in limited increases in mean prey abundance but greater increases in maximum prey abundance (i.e., mean value of highest 1% of habitat quality cells for the respective phosphorus load and meteorological year, Fig. 4). Maximum large zooplankton biomass demonstrated a linear, but variable response to increases in phosphorus,

with inconsequential to modest increases from 0.1-1.9 × phosphorus loads across meteorological years (range 0.4-20 %, Fig. 4b). Maximum chironomid biomass varied among meteorological years and increased non-linearly with increasing phosphorous loading, similar to that of hypoxia extent. While chironomid biomass was not directly affected by hypoxia, chironomid biomass responded as greater phosphorous loading contributed to greater carbon settling rates (range 18-27%, Fig. 4c).

Throughout the example 2002 meteorological year, habitat quality (GRP) responses of species and life-stages to phosphorus loading demonstrated seasonal effects of altered phosphorus loading (Fig. 5). While increasing phosphorus loading caused an increase in the duration and vertical extent of the hypoxic zone, higher phosphorus loading positively affected GRP slightly for all species and life-stages in early and mid-summer in the middle of the water column. Under low loading factor (× 0.1), annual peak GRP for adult yellow perch and rainbow smelt occurred in the bottom of the water column in late summer or early fall; however, at higher phosphorus loadings, the earlier development of the hypoxic zone appeared to overlap this spatiotemporal zone and peak GRP values appeared earlier in the year (early June) and higher in the water column.

Increasing phosphorus loading decreased or did not affect annual metrics of overall habitat quality (i.e., percentage of positive GRP and average GRP; Fig. 6, S9) depending on species and life-stage. Higher loading factors generally resulted in a decrease in percentage of positive GRP cells for adult rainbow smelt and adult round goby (Fig. 6). Therefore, modeled species and life-stages with relatively narrow, cold thermal preferences (e.g., adult rainbow smelt) or those restricted to demersal habitat (i.e., round goby) experienced a consistent decline in overall habitat quality with increasing phosphorus. Species and life-stages that do not rely as heavily on the hypolimnion for high quality habitat (e.g., adult emerald shiner) did not experience as significant of a disruption of overall habitat quality with increases in phosphorus and resulting hypoxia. Despite these responses to phosphorus loading, meteorological year appeared to be more influential in affecting both average annual GRP and percentage of positive cells (i.e., note spread in gray lines compared to change in black line in Fig. 6).

Annual indices of GRP-99% also responded to altered phosphorus loads, but responses were species- and life-stage-specific and sensitive to meteorological year (Fig. 7). Across years, pelagic species and life-stages that experienced peak habitat quality during peak zooplankton

production in June (i.e., young-of-year yellow perch, young-of-year rainbow smelt, and emerald shiners) exhibited increasing GRP-99% with increasing phosphorus loading. By contrast, pelagic and generalist species that benefit from chironomids in older life-stages (i.e., adult rainbow smelt, adult yellow perch) and benthic-oriented species (i.e., round goby) experienced sharp declines in GRP-99% at phosphorus levels which caused hypoxia to overlap with peak chironomid abundance, during a time when epilimnetic temperatures were relatively warm (Fig. S6; Fig. 5). Generally, highest GRP-99% was achieved at low phosphorus loadings for adult yellow perch, adult rainbow smelt, and round goby, but high loading maximized GRP-99% for young-of-year yellow perch, young-of-year rainbow smelt, and emerald shiner. Nonetheless, similar to other habitat quality indices, differences across loading scenarios were relatively small compared to differences in GRP-99% across different meteorological years (i.e., spread of gray lines in Fig. 7).

Diagnostic Application: Habitat quality trade-offs between hypoxia and prey

Diagnostic phosphorus response curve analyses to separately consider the influences of hypoxia and prey densities on habitat quality generally aligned with expectations and demonstrated the habitat quality trade-offs associated with increases in phosphorus; however, as demonstrated in the response curve analysis, variation in habitat quality metrics across meteorological years created more variability than the effects of phosphorus. Thus, the general trends from the analysis performed as expected and are described within this section, but meteorological conditions could more strongly affect habitat quality than a 1-year change in phosphorus loading (Fig. 8, S14-S19).

When we fixed oxygen concentrations to 10 mg $\cdot$ L^{-1} to focus on positive effects of increased loading leading to increased prey availability, annual GRP metrics indexing overall habitat quality (percentage of positive GRP and average GRP) and best habitat (GRP-99%) increased slightly with increasing phosphorus loads (Fig. 8, S14-S16). When we focused on potential negative effects of hypoxia by restricting daily mean prey biomass to levels obtained at 1.0 × phosphorous loading for each meteorological year, the model output demonstrated opposite patterns with percentage of positive GRP and average GRP declining across all species and life-stages as phosphorus load factor increased (Fig. 8, S17-S18). Under the assumption of prey biomass not responding to changes in phosphorus, GRP-99% responses differed across species

and life-stages, either not changing (young-of-year rainbow smelt), increasing (young-of-year yellow perch and adult emerald shiner) or declining (adult yellow perch, rainbow smelt, and round goby) in response to increased loading factor (Fig. S19). Increases or static changes in GRP-99% for species and life-stages reflected the influence of hypoxia on prey distributions. Although daily prey biomass did not change with increasing phosphorus loading factors, hypoxia still shifted zooplankton biomass higher in the water column increasing GRP-99% for species and life-stages that experienced their highest habitat quality above the hypolimnion (i.e., leading to increased GRP-99% for young-of-year yellow perch and adult emerald shiner despite no overall change in mean prey densities). The modeled output showed that overall habitat quality (percentage of positive GRP) of all species and life-stages was more responsive to the effect of hypoxia (Fig. 8, slope of blue dashed line closely matches black line). Prey fertilization did influence our modeled overall habitat quality (as demonstrated by the differences in blue and black lines in Fig. 8), but only slightly increased habitat quality at higher phosphorus loading factors.

Discussion

Simulation results demonstrated that there are species-specific habitat quality trade-offs between increased prey and hypoxia due to phosphorus loading. In total, model analyses agreed with our general hypotheses and confirm theoretical models and previous studies (Caddy, 1993, 2000; Arend *et al.*, 2011). However, our modeled results did not demonstrate the expected unimodal relationship between nutrient input and overall habitat quality (i.e., increase at low phosphorus levels, decrease at high phosphorus levels; Caddy, 1993; Rose *et al.*, 2018). Instead, our modeled output showed that at low phosphorus levels, increasing phosphorus led to increased habitat quality at particular depths and times of year. These favorable peaks of habitat quality (GRP-99%) declined precipitously for some species and life-stages, as the vertical extent and duration of hypoxia expanded. Declines in habitat quality with increasing phosphorus loading were particularly apparent for species and life-stages which otherwise benefitted from cool, bottom waters for suitable habitat and chironomid larvae as prey. Additionally, although we expected variability in annual meteorological conditions to affect the hypoxic zone (e.g., Lam *et al.*, 1987; Greene *et al.*, 2009; Deutsch *et al.*, 2011; Hughes *et al.*, 2015; Del Giudice *et al.*, 2018), we did not anticipate habitat quality to respond more strongly to meteorological year

conditions than to changes in phosphorus loading. Due to the complex influences of meteorological conditions, the analysis presented here suggests that short-term external phosphorus loading (i.e., a 1-year increase or decrease) has less of an influence than thermal and mixing regime on fish habitat quality, and thereby demonstrates how such interannual meteorological variability can obscure habitat responses to changes in phosphorus loading.

Habitat quality responses to phosphorus loading were species and life-stage specific

Our intra-annual results depicted as color-contour plots demonstrated mechanisms driving patterns of phosphorus benefitting (via a fertilization effect) and impairing (via hypoxia) habitat quality that have been observed and hypothesized in cross-system comparisons of fisheries responses to increased nutrients (Caddy, 1993, 2000; Rose *et al.*, 2019). Intra-annual results demonstrated how greater phosphorus loading increases prey density at particular times of year and depths of the water column, leading to higher GRP at those locations and time periods. This is reflected as increases in GRP-99% among years. However, if these areas were low enough in the water column, hypoxia eventually eliminated any benefit provided in that portion of the water column (e.g., adult yellow perch and rainbow smelt) leading to decreases in GRP-99% and counteracting gains in overall habitat quality (i.e., percentage of positive GRP). The loss of spatiotemporal occurrences of peak habitat quality can negatively affect growth and survival for specific species and life stages (Forsman & Lindell, 1991; Armstrong *et al.*, 2013, 2016; Murphy *et al.*, 2013; Baldock *et al.*, 2016); thus, inability to exploit hypolimnion habitat could have negative repercussions for populations even if overall habitat quality appears unaffected by increases in hypoxia. Fish population responses to nutrient loading can demonstrate this balancing effect between prey availability and hypoxia; however, as with our habitat quality results, responses varied by species and life-stages (Adamack *et al.*, 2017; Rose *et al.*, 2018).

The species- and life-stage- specific responses of habitat quality that our model results demonstrated align with empirical observations and previously modeled responses of pelagic-feeding species either benefitting by increased nutrients or not being affected by hypoxia (Zhang *et al.*, 2014; Adamack *et al.*, 2017), and benthic or benthopelagic species being negatively affected or emigrating in response to hypoxia (Howell & Simpson, 1994; Petersen & Pihl, 1995; Hughes *et al.*, 2015). The non-linear patterns of GRP-99% for the species and life-stages that use

the hypolimnion and feed preferentially on chironomids can be contrasted with the positive relationships between phosphorus loading and GRP-99% for species that benefitted more strongly from water column increases in zooplankton during early summer.

Responses in overall habitat quality (mean GRP and % positive cells) to phosphorous loading were species-specific, as demonstrated by primarily planktivorous species. Hypoxia negatively affected overall habitat quality for thermally sensitive adult rainbow smelt, while adult emerald shiner overall habitat quality appeared to be unaffected by hypoxia. These species-specific responses to hypoxia and phosphorus loading appear to be reflected in the distribution and abundance of rainbow smelt and emerald shiner in Lake Erie (Stone *et al.*, 2020). However, since our model did not incorporate concomitant changes in lower trophic level composition that could lead to inedible and toxin-producing forms of primary producers to dominate (Paerl & Fulton, 2006), our model results likely demonstrate simplified habitat responses. Future studies that examine the trade-offs associated with fish habitat quality responses to production and hypoxia could include greater recognition of associate changes in edibility and toxicity of primary producers and consequences for density and composition of primary and secondary consumers.

Meteorological variation and effect on habitat quality

Although meteorological variation has been shown to dramatically alter the extent and timing of hypoxia (Lam *et al.*, 1987; Deutsch *et al.*, 2011; Hughes *et al.*, 2015; Del Giudice *et al.*, 2018), the relationship between meteorological conditions and hypoxic extent does not necessarily explain why variation in GRP among meteorological years was greater than in response to altered phosphorus loading. Within the hindcast analysis, we found that zooplankton biomasses and temperature were more strongly correlated with our habitat quality metrics than hypoxia and total phosphorus loading for many species and life stages. This indicates that interannual changes in temperature, timing of nutrient loading and climatic conditions, as well as overall prey biomass may be more influential to cumulative habitat quality throughout the growing season than hypoxia. Additionally, the weak correlations between hypoxia and annual habitat quality metrics were positive for many species and life-stages in our hindcast analysis, suggesting that, rather than a negative effect of low oxygen, hypoxia may be an indicator for another change in habitat quality such as increased prey densities and redistribution of prey.

519 Within the response curve analyses, variation among years at the lowest loading factor (× 0.1)
520 when hypoxia was either absent or relatively brief was greater than the variation displayed across
521 all loading factors in the averaged response. If meteorological variation in hypoxic extent were
522 driving the interannual variation, we would expect the interannual variation at × 0.1 to be less
523 than that at higher phosphorus loadings, which modeled results did not consistently support. We
524 further confirmed that much of the variation among years was due to meteorological conditions
525 rather than hypoxic extent when we explored the effect of phosphorus on our annual GRP
526 metrics without the effect of dissolved oxygen. That is, the variation between meteorological
527 years persisted even when dissolved oxygen was not affecting habitat quality. These results
528 indicate that expected warming and shifts in precipitation patterns associated with climate
529 change will likely influence fish habitat quality by affecting the amount and timing of nutrient
530 loading (e.g., via increased extreme weather events, Michalak *et al.*, 2013), and by thermal
531 effects on organism physiology, prey availability and other habitat components. Overall, our
532 results suggest that meteorological conditions may be more influential to fish habitat quality than
533 total annual phosphorus loading, at least on short-term timelines.
534 The limited effect of phosphorus on habitat quality in comparison to meteorological
535 conditions may partially be related to the annual resetting of the input water quality model with a
536 set amount of phosphorus already in the system. Resetting our model with each nutrient ×
537 meteorological year did not allow us to explore the cumulative impact of increasing (or
538 decreasing) phosphorus across several consecutive years, meaning that internal phosphorus
539 loading (contributing up to 20% of external loading, Paytan *et al.*, 2017) likely buffered the
540 responses of both hypoxic extent and prey biomass to the changes in available nutrients. In
541 previous models, long-term (i.e., 20 + years) accumulation of nutrients had a stronger effect on
542 fish performance (Adamack *et al.*, 2017) than meteorological conditions, and decadal nutrient
543 loading rather than annual loading affected hypoxic extent (Del Giudice *et al.*, 2018). Thus, our
544 model is more representative of a 1-year change in phosphorus loading on habitat quality,
545 providing a short-term perspective on whether reducing nutrient loading can influence hypoxia
546 and fish habitat.
547 The seemingly low effect sizes of habitat quality responding to phosphorus loading that
548 we observed were partially due to our short-term perspective as well as our inclusion of an
549 almost full year (April – December) of GRP values. Similar GRP models (e.g., Brandt *et al.*,

2011; Stone *et al.*, 2020) have focused on the immediate time periods before, during, and after hypoxia, demonstrating how hypoxia alters habitat quality over 3 months. While including a greater proportion of the year may mute the apparent impact of hypoxia, our model allowed us to consider cumulative effects across a more realistic entire growing season. Ultimately, although our results do not exaggerate the influence of phosphorous loading on short-term habitat quality, they also demonstrate that environmental conditions such as temperature, vertical mixing, and light extinction on biological responses (e.g., prey timing and abundance, consumption, respiration) should not be overlooked when examining the effect of nutrients on overall and peak habitat quality. Climate change continues to alter aquatic habitats through changes in temperature and precipitation (Michalak *et al.*, 2013; Del Giudice *et al.*, 2018), which may be more influential on fish habitat quality than recent (< 10 years) changes in nutrient loading.

Study implications

Our model results reflect predicted habitat quality, but we believe they are also applicable and reflective of fish population responses to fertilization and hypoxia. Growth rate potential models are inherently difficult to validate. The intent of these models is to index habitat quality and not predict growth rates or spatial distributions. Fish are mobile and their growth rates reflect habitat use across many of our habitat "cells". GRP models do not track movement of individuals or include competition or other factors that influence habitat selection (Tyler & Brandt, 2001). Nonetheless, GRP measures appear to be related to performance (e.g., feeding, growth) of fish, are associated with vital rates of fish in natural systems, and demonstrate relative quality of habitats for populations (Brandt *et al.*, 1992; Tyler & Brandt, 2001). Past parameter perturbation analyses suggest that prediction uncertainty in bioenergetics models is influenced by different parameters in different species-specific models (Bartell *et al.*, 1986). In predicting growth, parameters related to consumption rate and inputs related to diet composition and energy densities have relatively greater influence (Bartell *et al.*, 1986). We did not explore changing these parameter values because these models have been developed and assessed in previous studies (Kitchell *et al.*, 1977; Hanson *et al.*, 1997; Duffy, 1998; Lee & Johnson, 2005) and a full sensitivity analysis was beyond the scope of the study. While parameter uncertainty can contribute to uncertainty in GRP calculations, GRP derived habitat quality is expected to relate to potential population performance after accounting for situations in which habitat quality and

density are not linked (e.g., if population sinks have strong influence; Van Horne, 1983; Pulliam, 1988). Previous GRP analyses performed with two of the species included in our analysis (i.e., rainbow smelt and emeral shiner) have demonstrated linkages between the effects of Lake Erie hypoxia on GRP habitat quality predictions, distribution and diet of fish, and long-term population trends (Stone *et al.*, 2020). Yellow perch population trends may be more complicated to infer from measures of habitat quality (i.e., GRP). Lake Erie yellow perch do migrate vertically or horizontally away from hypoxia; however, they also continue to forage on benthic chironomid larvae within hypoxic waters (Roberts *et al.*, 2009). Our model assumes that habitat quality below a certain oxygen threshold is not beneficial for yellow perch. Since yellow perch do continue to use this habitat via foraging forays (Roberts *et al.*, 2009) and juvenile hypoxia tolerance may be higher in cooler hypolimnion temperatures than we assumed in this model (Almeida *et al.*, 2017), annual GRP metrics may somewhat underestimate habitat quality for yellow perch adults and juveniles.

Overall, our results indicate that nutrient loading appears to increase the quantity of poor quality habitat, but potentially increases the quality of good habitat, which improves understanding of patterns observed across systems and via modeling exercises (Caddy, 2000; Breitburg *et al.*, 2009; Arend *et al.*, 2011; Adamack *et al.*, 2017; Rose *et al.*, 2019). This may benefit some populations (i.e., pelagic planktivores), but others may experience a greater mismatch with beneficial habitat conditions (i.e., benthic and bentho-pelagic fishes). Furthermore, results suggest that factors other than annual nutrient loading are more influential in determining overall habitat quality, which may indicate that evaluating the impact of nutrients on aquatic ecosystems may be obscured by inter-annual variation of various physio-chemical conditions. The strong effect of meteorological conditions on fish habitat quality suggests that ongoing changes in temperature and precipitation related to climatic change should be considered as both additive and interactive effects to understand how anthropogenic nutrient loading will continue to affect fish populations. Our results expand our understanding of how increases and decreases in nutrient loading may affect habitat quality through non-linear responses in hypoxic extent and prey densities. Understanding how environmental changes such as eutrophication dynamically affect habitat quality should improve the prediction of species responses and has the potential to inform the simultaneous management of fisheries and nutrient control programs.

Acknowledgements

We thank all those involved in the National Oceanic and Atmospheric Administration (NOAA) EcoFore-Lake Erie Project who provided data or modeling code, including Drs. Kristin Arend, Daisuke Goto, Dmitry Beletsky, Donald Scavia, Joe Depinto, and Stuart Ludsin. We also thank the Höök and Goforth labs at Purdue University for coding help and suggestions that improved the manuscript. This research was supported in part by the NOAA Center for Sponsored Coastal Ocean Research, Coastal Ocean Program grant NA07OAR432000 and a Knox Fellowship from Purdue University. This material is based upon work supported by the National Science Foundation Graduate Research Fellowship under Grant No.1333468. LZA, TMS, DKR, and TOH conceived of the study; LZA and TMS wrote the code and performed analyses with guidance from TOH; LZA drafted the manuscript with guidance and revisions from TMS, DKR, and TOH.

Data Availability Statement

Data and code will be made publicly available in the Purdue University Research Repository after acceptance of the manuscript.

References

Adamack A.T., Rose K.A. & Cerco C.F. (2017). Simulating the effects of nutrient loading rates and hypoxia on bay anchovy in Chesapeake Bay using coupled hydrodynamic, water quality, and individual-based fish models. In: *Modeling Coastal Hypoxia: Numerical Simulations of Patterns, Controls and Effects of Dissolved Oxygen Dynamics*. (Eds D. Justic, K.A. Rose, R.D. Hetland & K. Fennel), pp. 319–357. Springer International Publishing AG, Cham, Switzerland.

Almeida L.Z., Guffey S.C., Sepúlveda M.S. & Höök T.O. (2017). Behavioral and physiological responses of yellow perch (*Perca flavescens*) to moderate hypoxia. *Comparative Biochemistry and Physiology Part A: Molecular & Integrative Physiology* **209**, 47–55. https://doi.org/10.1016/j.cbpa.2017.04.009

641 Altieri A.H. & Diaz R.J. (2019). Dead zones: Oxygen depletion in coastal ecosystems. In: *World*
642 *Seas: An Environmental Evaluation Volume III: Ecological Issues and Environmental*
643 *Impacts*, Second Edi. (Ed. C. Sheppard), pp. 453–473. Elsevier Ltd.

644 Arend K.K., Beletsky D., DePinto J. V., Ludsin S.A., Roberts J.J., Rucinski D.K., *et al.* (2011).
645 Seasonal and interannual effects of hypoxia on fish habitat quality in central Lake Erie.
646 *Freshwater Biology* **56**, 366–383. https://doi.org/10.1111/j.1365-2427.2010.02504.x

647 Armstrong J.B., Schindler D.E., Ruff C.P., Brooks G.T., Bentley K.E. & Torgersen C.E. (2013).
648 Diel horizontal migration in streams: Juvenile fish exploit spatial heterogeneity in thermal
649 and trophic resources. *Ecology* **94**, 2066–2075. https://doi.org/10.1890/12-1200.1

650 Armstrong J.B., Takimoto G., Schindler D.E., Hayes M.M. & Kauffman M.J. (2016). Resource
651 waves: Phenological diversity enhances foraging opportunities for mobile consumers.
652 *Ecology* **97**, 1099–1112. https://doi.org/10.1890/15-0554.1/suppinfo

653 Avramidis P., Bekiari V., Christodoulou D. & Papatheodorou G. (2015). Sedimentology and
654 water column stratification in a permanent anoxic Mediterranean lagoon environment,
655 Aetoliko Lagoon, western Greece. *Environmental Earth Sciences* **73**, 5687–5701.
656 https://doi.org/10.1007/s12665-014-3824-2

657 Baldock J.R., Armstrong J.B., Schindler D.E. & Carter J.L. (2016). Juvenile coho salmon track a
658 seasonally shifting thermal mosaic across a river floodplain. *Freshwater Biology* **61**, 1454–
659 1465. https://doi.org/10.1111/fwb.12784

660 Baldwin C.M., Beauchamp D.A. & Gubala C.P. (2002). Seasonal and diel distribution and
661 movement of cutthroat trout from ultrasonic telemetry. *Transactions of the American*
662 *Fisheries Society* **131**, 143–158

663 Bartell S.M., Breck J.E., Gardner R.H. & Brenkert A.L. (1986). Individual parameter peturbation
664 and error analysis of fish bioenergetics models. *Canadian Journal of Fisheries and Aquatic*
665 *Sciences* **43**, 160–168. https://doi.org/10.1139/f86-018

666 Blaxter J.H.S. (1986). Development of sense organs and behavior of teleost larvae with special
667 reference to feeding and predator avoidance. *Transactions of the American Fisheries*
668 *Society* **115**, 98–114. https://doi.org/10.1577/1548-8659(1986)115

669 Blumenshine S.C., Vadeboncoeur Y., Lodge D.M., Cottingham K.L. & Knight S.E. (1997).
670 Benthic-pelagic links: responses of benthos to water-column nutrient enrichment. *Journal of*
671 *the North American Benthological Society* **16**, 466–479. https://doi.org/10.2307/1468138

672 Bocaniov S.A. & Scavia D. (2016). Temporal and spatial dynamics of large lake hypoxia:
673 Integrating statistical and three-dimensional dynamic models to enhance lake management
674 criteria. *Water Resources Research* **52**, 4247–4263. https://doi.org/10.1002/2015WR018170

675 Brandt S.B. (1993). The effect of thermal fronts on fish growth: a bioenergetic evaluation of food
676 and temperature. *Estuaries* **16**, 142–159

677 Brandt S.B., Costantini M., Kolesar S., Ludsin S.A., Mason D.M., Rae C.M., *et al.* (2011). Does
678 hypoxia reduce habitat quality for Lake Erie walleye (Sander vitreus)? A bioenergetics
679 perspective. *Canadian Journal of Fisheries and Aquatic Sciences* **68**, 857–879.
680 https://doi.org/10.1139/f2011-018

681 Brandt S.B., Mason D.M. & Patrick E.V. (1992). Spatially-explicit models of fish growth rate.
682 *Fisheries* **17**, 23–35. https://doi.org/10.1577/1548-
683 8446(1992)017<0023:SMOFGR>2.0.CO;2

684 Breck J.E. (1993). Hurry up and wait: Growth of young bluegills in ponds and in simulations
685 with an individual-based model. *Transactions of the American Fisheries Society* **122**, 467–
686 480. https://doi.org/10.1577/1548-8659(1993)122<0467:HUAWGO>2.3.CO;2

687 Breck J.E. & Gitter M.J. (1983). Effect of fish size on the reactive distance of bluegill (Lepomis
688 macrochirus) sunfish. *Canadian Journal of Fisheries and Aquatic Sciences* **40**, 162–167.
689 https://doi.org/10.1139/f83-026

690 Breitburg D. (2002). Effects of hypoxia, and the balance between hypoxia and enrichment, on
691 coastal fishes and fisheries. *Estuaries* **25**, 767–781. https://doi.org/10.1007/BF02804904

692 Breitburg D.L., Hondorp D.W., Davias L.A. & Diaz R.J. (2009). Hypoxia, nitrogen, and
693 fisheries: Integrating effects across local and global landscapes. *Annual Review of Marine*
694 *Science* **1**, 329–349. https://doi.org/10.1146/annurev.marine.010908.163754

695 Budy P., Baker M. & Dahle S.K. (2011). Predicting fish growth potential and identifying water
696 quality constraints: A spatially-explicit bioenergetics approach. *Environmental Management*

48, 691–709. https://doi.org/10.1007/s00267-011-9717-1

Burns N.M., Rockwell D.C., Bertram P.E., Dolan D.M. & Ciborowski J.J.H. (2005). Trends in temperature, secchi depth, and dissolved oxygen depletion rates in the central basin of Lake Erie, 1983–2002. *Journal of Great Lakes Research* **31**, 35–49. https://doi.org/10.1016/S0380-1330(05)70303-8

Caddy J.F. (2000). Marine catchment basin effects versus impacts of fisheries on semi-enclosed seas. *ICES Journal of Marine Science* **57**, 628–640. https://doi.org/10.1006/jmsc.2000.0739

Caddy J.F. (1993). Toward a comparative evaluation of human impacts on fishery ecosystems of enclosed and semi-enclosed seas. *Reviews in Fisheries Science* **1**, 57–95

Deutsch C., Brix H., Ito T., Frenzel H. & Thompson L. (2011). Climate-forced variability of ocean hypoxia. *Science* **333**, 336–339

Diaz R.J. (2001). Overview of hypoxia around the world. *Journal of Environmental Quality* **30**, 275–281. https://doi.org/10.2134/jeq2001.302275x

Diaz R.J. & Rosenberg R. (2008). Spreading dead zones and consequences for marine ecosystems. *Science* **321**, 926–929. https://doi.org/10.1126/science.1156401

Duffy W.G. (1998). Population dynamics, production, and prey consumption of fathead minnows (Pimephales promelas) in prairie wetlands: a bioenergetics approach. *Canadian Journal of Fisheries and Aquatic Sciences* **55**, 15–27. https://doi.org/10.1139/cjfas-55-1-15

Eby L.A., Crowder L.B., McClellan C.M., Peterson C.H. & Powers M.J. (2005). Habitat degradation from intermittent hypoxia: Impacts on demersal fishes. *Marine Ecology Progress Series* **291**, 249–261

Elmgren R. (1989). Man's impact on the ecosystem of the Baltic Sea: Energy flows today and at the turn of the century. *Ambio* **18**, 326–332

Forsman A. & Lindell L.E. (1991). Trade-off between growth and energy storage in male Vipera berus (L.) under different prey densities. *Functional Ecology* **5**, 717–723. https://doi.org/10.2307/2389533

Fulford R.S., Rice J.A., Miller T.J., Binkowski F.P., Dettmers J.M. & Belonger B. (2006).

Foraging selectivity by larval yellow perch (Perca flavescens): Implications for understanding recruitment in small and large lakes. *Canadian Journal of Fisheries and Aquatic Sciences* **63**, 28–42. https://doi.org/10.1139/f05-196

Del Giudice D., Fang S., Scavia D., Davis T.W., Evans M.A. & Obenour D.R. (2021). Elucidating controls on cyanobacteria bloom timing and intensity via Bayesian mechanistic modeling. *Science of the Total Environment* **755**, 142487. https://doi.org/10.1016/j.scitotenv.2020.142487

Del Giudice D., Zhou Y., Sinha E. & Michalak A.M. (2018). Long-term phosphorus loading and springtime temperatures explain interannual variability of hypoxia in a large temperate lake. *Environmental Science and Technology* **52**, 2046–2054. https://doi.org/10.1021/acs.est.7b04730

Glaspie C.N., Clouse M., Huebert K., Ludsin S.A., Mason D.M., Pierson J.J., *et al.* (2019). Fish diet shifts associated with the northern Gulf of Mexico hypoxic zone. *Estuaries and Coasts* **42**, 2170–2183. https://doi.org/10.1007/s12237-019-00626-x

Goto D., Roberts J.J., Pothoven S.A., Ludsin S.A., Vanderploeg H.A., Brandt S.B., *et al.* (2017). Size-mediated control of perch–midge coupling in Lake Erie transient dead zones. *Environmental Biology of Fishes* **100**, 1587–1600. https://doi.org/10.1007/s10641-017-0667-1

Graeb B.D.S., Dettmers J.M., Wahl D.H. & Cáceres C.E. (2004). Fish size and prey availability affect growth, survival, prey selection, and foraging behavior of larval yellow perch. *Transactions of the American Fisheries Society* **133**, 504–514. https://doi.org/10.1577/T03-050.1

Greene R.M., Lehrter J.C. & Hagy J.D. (2009). Multiple regression models for hindcasting and forecasting midsummer hypoxia in the Gulf of Mexico. *Ecological Applications* **19**, 1161–1175. https://doi.org/10.1890/08-0035.1

Hanson P.C., Johnson T.B., Schindler D.E. & Kitchell J.F. (1997). *Fish bioenergetics 3.0 for Windows*.

Harris Geospatial Solutions Inc. (2019). Interactive Data Language

Hergenrader G.L. & Hasler A.D. (1967). Seasonal changes in swimming rates of yellow perch in Lake Mendota as measured by sonar. *Transactions of the American Fisheries Society* **96**, 373–382

Van Horne B. (1983). Density as a misleading indicator of habitat quality. *The Journal of Wildlife Management* **47**, 893–901

Howell P. & Simpson D. (1994). Abundance of marine resources in relation to dissolved oxygen in Long Island Sound. *Estuaries* **17**, 394. https://doi.org/10.2307/1352672

Hrycik A.R., Almeida L.Z. & Höök T.O. (2017). Sub-lethal effects on fish provide insight into a biologically-relevant threshold of hypoxia. *Oikos* **126**, 307–317. https://doi.org/10.1111/oik.03678

Hughes B.B., Levey M.D., Fountain M.C., Carlisle A.B., Chavez F.P. & Gleason M.G. (2015). Climate mediates hypoxic stress on fish diversity and nursery function at the land–sea interface. *Proceedings of the National Academy of Sciences* **112**, 8025–8030. https://doi.org/10.1073/pnas.1505815112

Jensen O.P., Hansson S., Didrikas T., Stockwell J.D., Hrabik T.R., Axenrot T., *et al.* (2011). Foraging, bioenergetic and predation constraints on diel vertical migration: Field observations and modelling of reverse migration by young-of-the-year herring *Clupea harengus*. *Journal of Fish Biology* **78**, 449–465. https://doi.org/10.1111/j.1095-8649.2010.02855.x

Kassambara A. (2020). ggpubr: "ggplot2" Based Publication Ready Plots

Kirk J.T.O. (1977). Attenuation of light in natural waters. *Australian Journal of Marine and Freshwater Research* **28**, 497–508. https://doi.org/10.1039/c2ay25041a

Kitchell J.F., Stewart D.J. & Weininger D. (1977). Applications of a bioenergetics model to yellow perch (Perca flavescens) and walleye (Stizostedion vitreum vitreum). *Journal of the Fisheries Research Board of Canada* **34**, 1922–1935

Kraus R.T., Knight C.T., Farmer T.M., Gorman A.M., Collingsworth P.D., Warren G.J., *et al.* (2015). Dynamic hypoxic zones in Lake Erie compress fish habitat, altering vulnerability to fishing gears. *Canadian Journal of Fisheries and Aquatic Sciences* **72**, 797–806.

https://doi.org/10.1139/cjfas-2014-0517

Kuiper J.J., van Altena C., de Ruiter P.C., van Gerven L.P.A., Janse J.H. & Mooij W.M. (2015). Food-web stability signals critical transitions in temperate shallow lakes. *Nature Communications* **6**, 7727. https://doi.org/10.1038/ncomms8727

Lam D.C.L., Schertzer W.M. & Fraser A.S. (1987). A post-audit anaylsis of the NWRI nine-box water quality model for Lake Erie. *Journal of Great Lakes Research* **13**, 782–800. https://doi.org/10.1016/S0380-1330(87)71691-8

Lee V.A. & Johnson T.B. (2005). Development of a bioenergetics model for the round goby (Neogobius melanostomus). *Journal of Great Lakes Research* **31**, 125–134. https://doi.org/10.1016/S0380-1330(05)70244-6

Ludsin S.A., Kershner M.W., Blocksom K.A., Knight R. & Stein R.A. (2001). Life after death in Lake Erie: Nutrient controls drive fish species richness, rehabilitation. *Ecological Applications* **11**, 731–746. https://doi.org/10.1890/1051-0761(2001)011

Ludsin S.A., Zhang X., Brandt S.B., Roman M.R., Boicourt W.C., Mason D.M., *et al.* (2009). Hypoxia-avoidance by planktivorous fish in Chesapeake Bay: Implications for food web interactions and fish recruitment. *Journal of Experimental Marine Biology and Ecology* **381**, 121–131. https://doi.org/10.1016/j.jembe.2009.07.016

Lyche Solheim A., Rekolainen S., Moe S.J., Carvalho L., Phillips G., Ptacnik R., *et al.* (2008). Ecological threshold responses in European lakes and their applicability for the Water Framework Directive (WFD) implementation: Synthesis of lakes results from the REBECCA project. *Aquatic Ecology* **42**, 317–334. https://doi.org/10.1007/s10452-008-9188-5

Makarewicz J.C., Lewis T.W. & Bertram P. (1989). *Phytoplankton and zooplankton composition, abundance and distribution and trophic interactions: Offshore region of Lakes Erie, Lake Huron and Lake Michigan, 1985*.

May C.J., Aday D.D., Hale R.S., Denlinger J.C.S. & Marschall E.A. (2012). Modeling habitat selection of a top predator: Considering growth and physical environments in a spatial context. *Transactions of the American Fisheries Society* **141**, 215–223.

https://doi.org/10.1080/00028487.2012.655122

Michalak A.M., Anderson E.J., Beletsky D., Boland S., Bosch N.S., Bridgeman T.B., *et al.* (2013). Record-setting algal bloom in Lake Erie caused by agricultural and meteorological trends consistent with expected future conditions. *Proceedings of the National Academy of Sciences of the United States of America* **110**, 6448–6452. https://doi.org/10.1073/pnas.1216006110

Murphy H.M., Jenkins G.P., Hamer P.A. & Swearer S.E. (2013). Interannual variation in larval abundance and growth in snapper *Chrysophrys auratus* (Sparidae) is related to prey availability and temperature. *Marine Ecology Progress Series* **487**, 151–162. https://doi.org/10.3354/meps10388

Ohio DOW (2020). *Ohio's Lake Erie Fisheries: 2019 Annual Report*.

Paerl H.W. & Fulton R.S. (2006). Ecology of harmful cyanobacteria. In: *Ecology of Harmful Algae*. pp. 95–109.

Paytan A., Roberts K., Watson S., Peek S., Chuang P.-C., Defforey D., *et al.* (2017). Internal loading of phosphate in Lake Erie Central Basin. *Science of the Total Environment* **579**, 1356–1365. https://doi.org/10.1016/j.scitotenv.2016.11.133

Petersen J.K. & Pihl L. (1995). Responses to hypoxia of plaice, Pleuronectes platessa, and dab, Limanda limanda, in the south-east Kattegat: distribution and growth. *Environmental Biology of Fishes* **43**, 311–321. https://doi.org/10.1007/BF00005864

Pihl L. (1994). Changes in the diet of demersal fish due to eutrophication-induced hypoxia in the Kattegat, Sweden. *Canadian Journal of Fisheries and Aquatic Sciences* **51**, 321–336. https://doi.org/10.1139/f94-033

Pihl L., Baden S.P. & Diaz R.J. (1991). Effects of periodic hypoxia on distribution of demersal fish and crustaceans. *Marine Biology* **108**, 349–360

Pollock M.S., Clarke L.M.J. & Dubé M.G. (2007). The effects of hypoxia on fishes: From ecological relevance to physiological effects. *Environmental Reviews* **15**, 1–14. https://doi.org/10.1139/a06-006

Pothoven S.A., Vanderploeg H.A., Ludsin S.A., Höök T.O. & Brandt S.B. (2009). Feeding

836 ecology of emerald shiners and rainbow smelt in central Lake Erie. *Journal of Great Lakes*
837 *Research* **35**, 190–198. https://doi.org/10.1016/j.jglr.2008.11.011

838 Pulliam H.R. (1988). Sources, sinks, and population regulation. *The American Naturalist* **132**,
839 652–661

840 R Core Team (2021). R: A Language and Environment for Statistical Computing

841 Roberts J.J., Höök T.O., Ludsin S.A., Pothoven S.A., Vanderploeg H.A. & Brandt S.B. (2009).
842 Effects of hypolimnetic hypoxia on foraging and distributions of Lake Erie yellow perch.
843 *Journal of Experimental Marine Biology and Ecology* **381**.
844 https://doi.org/10.1016/j.jembe.2009.07.017

845 Rose K.A., Creekmore S., Justić D., Thomas P., Craig J.K., Neilan R.M., *et al.* (2018). Modeling
846 the population effects of hypoxia on Atlantic croaker (*Micropogonias undulatus*) in the
847 northwestern Gulf of Mexico: Part 2—Realistic hypoxia and eutrophication. *Estuaries and*
848 *Coasts* **41**, 255–279. https://doi.org/10.1007/s12237-017-0267-5

849 Rose K.A., Gutiérrez D., Breitburg D., Conley D., Craig K.J., Froehlich H.E., *et al.* (2019).
850 Impacts of ocean deoxygenation on fisheries. In: *Ocean deoxygenation: Everyone's*
851 *problem Causes, impacts, consequences and solutions*. (Eds D. Laffoley & J.M. Baxter), pp.
852 519–544. International Union for Conservation of Nature - Global Marine and Polar
853 Programme.

854 Rose K.A., Rutherford E.S., Mcdermot D.S., Forney J.L. & Mills E.L. (1999). Individual-based
855 model of yellow perch and walleye populations in Oneida Lake. *Ecological Monographs*
856 **69**, 127–154

857 Rose K.A., Tyler J.A., Chambers R.C., Klein-MacPhee G. & Danila D.J. (1996). Simulating
858 winter flounder population dynamics using coupled individual-based young-of-the-year and
859 age-structured adult models. *Canadian Journal of Fisheries and Aquatic Sciences* **53**, 1071–
860 1091. https://doi.org/10.1139/f96-031

861 Rucinski D.K., DePinto J. V., Scavia D. & Beletsky D. (2014). Modeling Lake Erie's hypoxia
862 response to nutrient loads and physical variability. *Journal of Great Lakes Research* **40**,
863 151–161. https://doi.org/10.1016/j.jglr.2014.02.003

Scavia D., Allan J.D., Arend K.K., Bartell S., Beletsky D., Bosch N.S., *et al.* (2014). Assessing and addressing the re-eutrophication of Lake Erie: Central basin hypoxia. *Journal of Great Lakes Research* **40**, 226–246. https://doi.org/10.1016/j.jglr.2014.02.004

Scavia D., DePinto J. V. & Bertani I. (2016). A multi-model approach to evaluating target phosphorus loads for Lake Erie. *Journal of Great Lakes Research* **42**, 1139–1150. https://doi.org/10.1016/j.jglr.2016.09.007

Shoji J., Masuda R., Yamashita Y. & Tanaka M. (2005). Effect of low dissolved oxygen concentrations on behavior and predation rates on red sea bream Pagrus major larvae by the jellyfish Aurelia aurita and by juvenile Spanish mackerel Scomberomorus niphonius. *Marine Biology* **147**, 863–868. https://doi.org/10.1007/s00227-005-1579-8

Silva N. & Vargas C.A. (2014). Hypoxia in Chilean Patagonian fjords. *Progress in Oceanography* **129**, 62–74. https://doi.org/10.1016/j.pocean.2014.05.016

Smith S. V, Kimmerer W.J., Laws E.A., Brock R.E. & Walsh T.W. (1981). Kaneohe Bay sewage diversion experiment: Perspectives on ecosystem responses to nutritional perturbation. *Pacific Science* **35**, 279–395

Stone J.P., Pangle K.L., Pothoven S.A., Vanderploeg H.A., Brandt S.B., Höök T.O., *et al.* (2020). Hypoxia's impact on pelagic fish populations in Lake Erie: A tale of two planktivores. *Canadian Journal of Fisheries and Aquatic Sciences* **18**, 1–18. https://doi.org/10.1139/cjfas-2019-0265

Systat Software Inc. (2017). SigmaPlot

Trolle D., Skovgaard H. & Jeppesen E. (2008). The Water Framework Directive: Setting the phosphorus loading target for a deep lake in Denmark using the 1D lake ecosystem model DYRESM-CAEDYM. *Ecological Modelling* **219**, 138–152. https://doi.org/10.1016/j.ecolmodel.2008.08.005

Tyler J.A. & Brandt S.B. (2001). Do spatial models of growth rate potential reflect fish growth in a heterogeneous environment? A comparison of model results. *Ecology of Freshwater Fish* **10**, 43–56. https://doi.org/10.1034/j.1600-0633.2001.100106.x

Vanderploeg H.A., Ludsin S.A., Ruberg S.A., Höök T.O., Pothoven S.A., Brandt S.B., *et al.*

(2009). Hypoxia affects spatial distributions and overlap of pelagic fish, zooplankton, and phytoplankton in Lake Erie. *Journal of Experimental Marine Biology and Ecology* **381**, S92–S107. https://doi.org/10.1016/j.jembe.2009.07.027

Wickham H. (2016). *ggplot2: Elegant Graphics for Data Analysis*. Springer-Verlag New York.

Wilke C.O. (2020). cowplot: Streamlined Plot Theme and Plot Annotations for "ggplot2"

Zhang H., Mason D.M., Stow C.A., Adamack A.T., Brandt S.B., Zhang X., *et al.* (2014). Effects of hypoxia on habitat quality of pelagic planktivorous fishes in the northern gulf of Mexico. *Marine Ecology Progress Series* **505**, 209–226. https://doi.org/10.3354/meps10768

Zhang J., Gilbert D., Gooday A.J., Levin L., Naqvi S.W.A., Middelburg J.J., *et al.* (2010). Natural and human-induced hypoxia and consequences for coastal areas: Synthesis and future development. *Biogeosciences* **7**, 1443–1467. https://doi.org/10.5194/bg-7-1443-2010

Supporting Information

Appendix S1: Methods on prey abundance and distribution methods, growth rate potential calculations, and foraging sub-model calculations. Results of intra-annual responses, GRP-95%, and model assessments of DO and prey.

Table S1: Focal fish species bioenergetics model parameter estimates.

Table S2: Half saturation constants (k, no. prey $\cdot$ s^{-1}) for all prey types for each species and age class.

Table S3: Prey selectivity values and equations for all prey types for each species and age class.

Figure S1: Graphical depictions of the temperature, light, and DO functions in zooplankton redistribution.

Figure S2: Temperature-based survival developed from published experiments.

Figure S3: Comparison of observed chironomid larvae biomass during field sampling and modeled chironomid larvae biomass.

Figure S4: Lengths observed from field collections of chironomid larvae used to interpolate lengths of chironomid prey in the foraging sub-model.

Figure S5: Daily changes in physical and biological variables and in GRP for the day of September 15, 2002.

Figure S6: Physical and biological variables at different time periods throughout the year.

Figure S7: GRP ($g \cdot g^{-1} \cdot d^{-1}$) at different time periods throughout the year.

Figure S8: Prey densities of large zooplankton ($mg \cdot L^{-1}$) at four time periods throughout 2002 and of chironomidae larvae $g \cdot m^{-2}$ throughout 2002 at various phosphorus loads.

Figure S9: Spatiotemporal habitat cells included in the GRP-99% calculation for adult yellow perch, adult rainbow smelt, and adult emerald shiner in 2002.

Figure S10: Spatiotemporal habitat cells included in the GRP-99% calculation for adult yellow perch throughout 2002 and at four time-step throughout the day.

Figure S11: Spatiotemporal habitat cells included in the GRP-95% calculation for adult yellow perch throughout 2002 and at four time-step throughout the day.

Figure S12: The effect of increasing phosphorus on GRP-95%.

Figure S13: The effect on increasing phosphorus on average GRP.

Figure S14: The effect on increasing phosphorus on percentage of positive GRP cells when DO was restricted to 10 $mg \cdot L^{-1}$.

Figure S15: The effect on increasing phosphorus on average GRP when DO was restricted to 10 $mg \cdot L^{-1}$.

Figure S16: The effect on increasing phosphorus on GRP-99% when DO was restricted to 10 $mg \cdot L^{-1}$.

Figure S17: The effect on increasing phosphorus on percentage of positive GRP cells when prey biomasses were restricted to the prey biomasses at × 1.0 loading factor for each meteorological year.

Figure S18: The effect on increasing phosphorus on average GRP when prey biomasses were restricted to the prey biomasses at × 1.0 loading factor for each meteorological year.

Figure S19: The effect on increasing phosphorus on GRP-99% when prey biomasses were restricted to the prey biomasses at × 1.0 loading factor for each meteorological year.

Tables

951 Table 1: Meteorological year data and phosphorus loading factors used for each GRP model
952 scenario.

Scenario	Meteorological Year	Phosphorus Loading Year	Total GRP years simulated
Hindcast	1987 – 2005	1987 – 2005	19
Phosphorus Response Curves	1987 – 2005	0.1 – 1.9 × phosphorus loads of 1997	361
Diagnostic Application			
Fixed oxygen	1987 – 2005	0.1 – 1.9 × phosphorus loads of 1997	361
Fixed proportion of max consumption	1987 – 2005	0.1 – 1.9 × phosphorus loads of 1997	361

953
954
955 Table 2: Spearman rank correlation coefficients (ρ) for relationships between pairs of annual
956 values of biotic and abiotic habitat characteristics and two modeled habitat quality metrics
957 (percentage of positive GRP and GRP-99%) in the hindcast simulation (n = 19 years). Biotic and
958 abiotic habitat characteristics include total phosphorus (TP), temperature (°C, Temp), number
959 hypoxia cells at ≤ 2.0 mg · L^{-1} (Hypoxia2), number of hypoxic cells at ≤ 4.0 mg · L^{-1} (Hypoxia4),
960 total zooplankton biomass (mg · L^{-1} , ZP Bio), and total chironomid biomass (g · L^{-1}, Chiro Bio).
961 Modeled habitat quality metrics include the annual growth rate potential (GRP) indices
962 percentage of positive GRP (PP GRP) and GRP-99% for all species and life stages. The species
963 codes are as follows: ES adult is adult emerald shiner, YP YOY is young-of-year yellow perch,
964 RS YOY is young-of-year rainbow smelt, YP adult is adult yellow perch, RS adult is adult
965 rainbow smelt, RG adult is adult round goby. Bolded values indicate strong correlations ($|\rho| \geq$
966 0.80) and underlined values indicate moderate to strong correlations ($|\rho| \geq 0.40$). * indicates that
967 the correlation was significant ($P < 0.05$).
968

	TP	Temp	Hypoxia2	Hypoxia4	ZP Bio	Chiro Bio
TP						
Temp	0.10					
Hypoxia2	0.37	0.56*				
Hypoxia4	0.25	0.43	**0.85***			
ZP Bio	0.05	-0.32	0.13	0.26		
Chiro Bio	0.47*	0.59*	**0.85***	0.66*	0.01	
PP YP YOY	0.03	-0.05	0.24	0.23	**0.87***	0.23
PP YP adult	0.06	-0.14	0.21	0.24	**0.90***	0.19
PP RS YOY	0.11	-0.03	0.34	0.38	**0.81***	0.35
PP RS adult	0.17	-0.48*	-0.03	0.13	**0.85***	-0.16
PP ES adult	0.16	-0.12	0.25	0.37	**0.92***	0.23
PP RG adult	0.04	0.43	0.10	-0.12	-0.19	0.30
GRP99 YP YOY	0.10	-0.35	0.00	0.10	0.78*	0.03
GRP99 YP adult	0.10	-0.47*	-0.05	0.11	**0.86***	-0.09
GRP99 RS YOY	0.08	-0.51*	-0.05	0.03	0.72*	-0.08
GRP99 RS adult	-0.03	-0.48*	-0.24	-0.29	0.66*	-0.28
GRP99 ES adult	0.16	-0.40	0.04	0.16	**0.84***	0.02
GRP99 RG adult	0.03	0.53*	0.11	-0.14	-0.33	0.39

Figure Legends

Figure 1: A schematic of the growth rate potential (GRP) model including input data from Rucinski *et al*. (2014), prey distributions sub-model, and bioenergetics sub-model (Appendix S1 pages 4-13). The calculation of consumption is performed in the foraging sub-model (Appendix S1 pages 13-19). Arrows indicate which model output or variables are used in the following model.

Figure 2: Growth rate potential (GRP) model output at various time scales. Adult yellow perch (YP adult) habitat quality (GRP) fluctuates seasonally, daily, and sub-daily due to changes in physical (e.g., light) and biological (e.g., large zooplankton) factors. These patterns are shown in a representative year (e.g., 2002) and, on a shorter time-scale, in a representative day (e.g.,

September 15, 2002). Note that the scale for the physical and biological factors on 15 September 2002 are shown in Appendix S1, Fig. S5 and runs from black (0) to white (highest values). The scale for adult yellow perch GRP is the scale used throughout the rest of the figure.

Figure 3: Results from the hindcast simulation demonstrating (a) mean annual temperatures (°C) and annual total phosphorus load (MT); (b) number of hypoxic cells (DO ≤ 2.0 and DO ≤ 4.0 mg · L^{-1}) per year; (c) total biomass of zooplankton (mg · L^{-1}) and chironomids (g · L^{-1}) per year; (d) percentage of positive GRP cells per year for all species and life-stages; (e) average GRP per year for all species and life-stages; (f) GRP-99% per year for all species and life-stages. The species codes are as follows: ES adult is adult emerald shiner, YP YOY is young-of-year yellow perch, RS YOY is young-of-year rainbow smelt, YP adult is adult yellow perch, RS adult is adult rainbow smelt, RG adult is adult round goby.

Figure 4: The effect of increasing phosphorus (x-axis) on (a) extent of hypoxia, (b) mean (gray and black) and maximum (i.e., mean of highest 1% of habitat cells, light and dark blue) large zooplankton biomass, (c) mean (gray and black) maximum (light and dark blue) chironomid biomass. Gray and light blue lines represent different meteorological years (1987 to 2005), and black or dark blue lines represent the mean across all meteorological years.

Figure 5: GRP (g · g^{-1} · d^{-1}) during midday represented as different colors for three phosphorus loads in three species and life-stages. Time throughout the representative year 2002 is portrayed along the x-axis, depth is represented as an inverted y-axis. Column (a) phosphorus × 0.1, (b) phosphorus × 1.0, (c) phosphorus × 1.9 of 1997's phosphorus loading (a moderate phosphorus loading year). Row 1) adult yellow perch (YP Adult), 2) adult rainbow smelt (RS Adult), 3) adult emerald shiner (ES Adult).

Figure 6: The effect of increasing phosphorus (x-axis) on relative percentage change in percentage of positive GRP cells (y-axis) for each species and life stage: young-of-year yellow perch (a, YP YOY), young-of-year rainbow smelt (b, RS YOY), adult emerald shiner (c, ES Adult), adult yellow perch (d, YP Adult), adult rainbow smelt (e, RS Adult), adult round goby (f, RG Adult). Percent changed was relativized to the mean percentage of positive GRP cells

achieved across all meteorological years at 1.0 × phosphorus loading for each species and life-stage. Solid gray lines represent different meteorological years (1987 to 2005) and solid black lines represent the mean across all meteorological years.

Figure 7: The effect of increasing phosphorus (x-axis) on relative percentage change in GRP-99% (y-axis) for each species and life stage: young-of-year yellow perch (a, YP YOY), young-of-year rainbow smelt (b, RS YOY), adult emerald shiner (c, ES Adult), adult yellow perch (d, YP Adult), adult rainbow smelt (e, RS Adult), adult round goby (f, RG Adult). Percent changed was relativized to the mean GRP-99% achieved across all meteorological years at 1.0 × phosphorus loading for each species and life-stage. Solid gray lines represent different meteorological years (1987 to 2005) and solid black lines represent the mean across all meteorological years.

Figure 8: The effect of increasing phosphorus (x-axis) on relative percentage change in percentage of positive GRP cells (y-axis) when phosphorus increases hypoxia and prey (solid black line – Response Curves), only increases prey (orange dash-dot line – Diagnostic Application), or only increases hypoxia (blue dashed line – Diagnostic Application). Lines represent mean relative precent change across all 19 meteorological years, with data relativized to the mean percentage of positive GRP cells achieved across all meteorological years at 1.0 × phosphorus loading. Shaded areas indicate standard error (SE) of the mean across meteorological years, with shaded coloring paired with line color. Each species and life-stage is represented: young-of-year yellow perch (a, YP YOY), young-of-year rainbow smelt (b, RS YOY), adult emerald shiner (c, ES Adult), adult yellow perch (d, YP Adult), adult rainbow smelt (e, RS Adult), adult round goby (f, RG Adult).

Figure 1

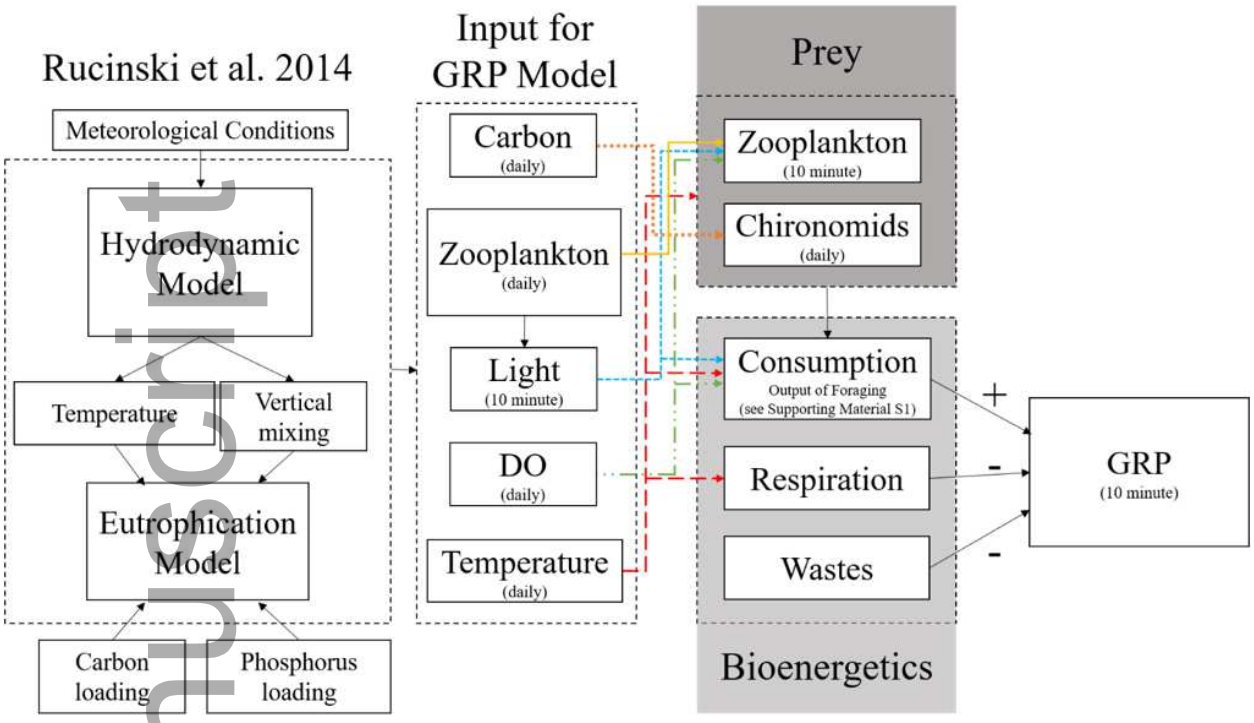

Figure 2

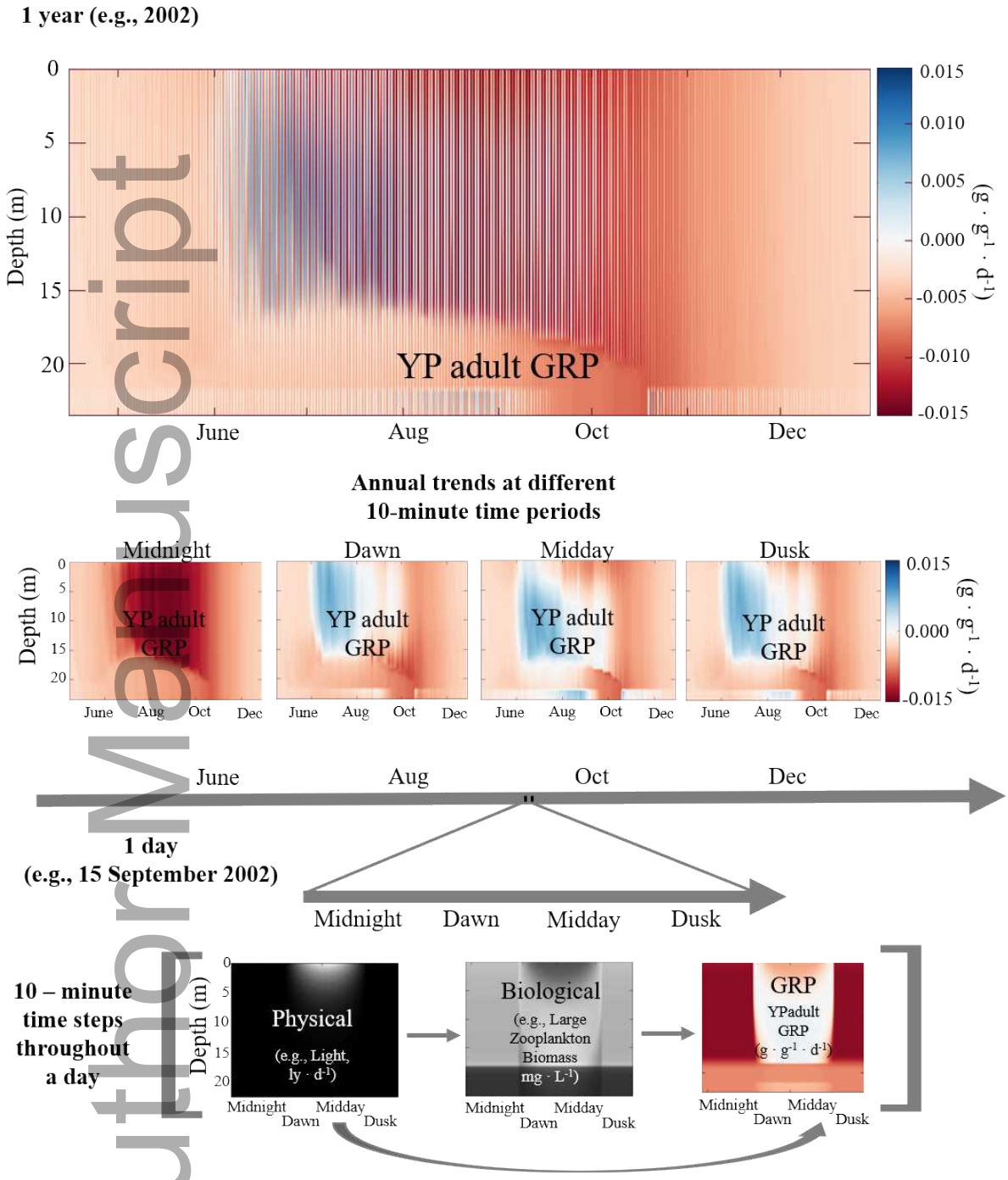

1041

1042

1043 Figure 3

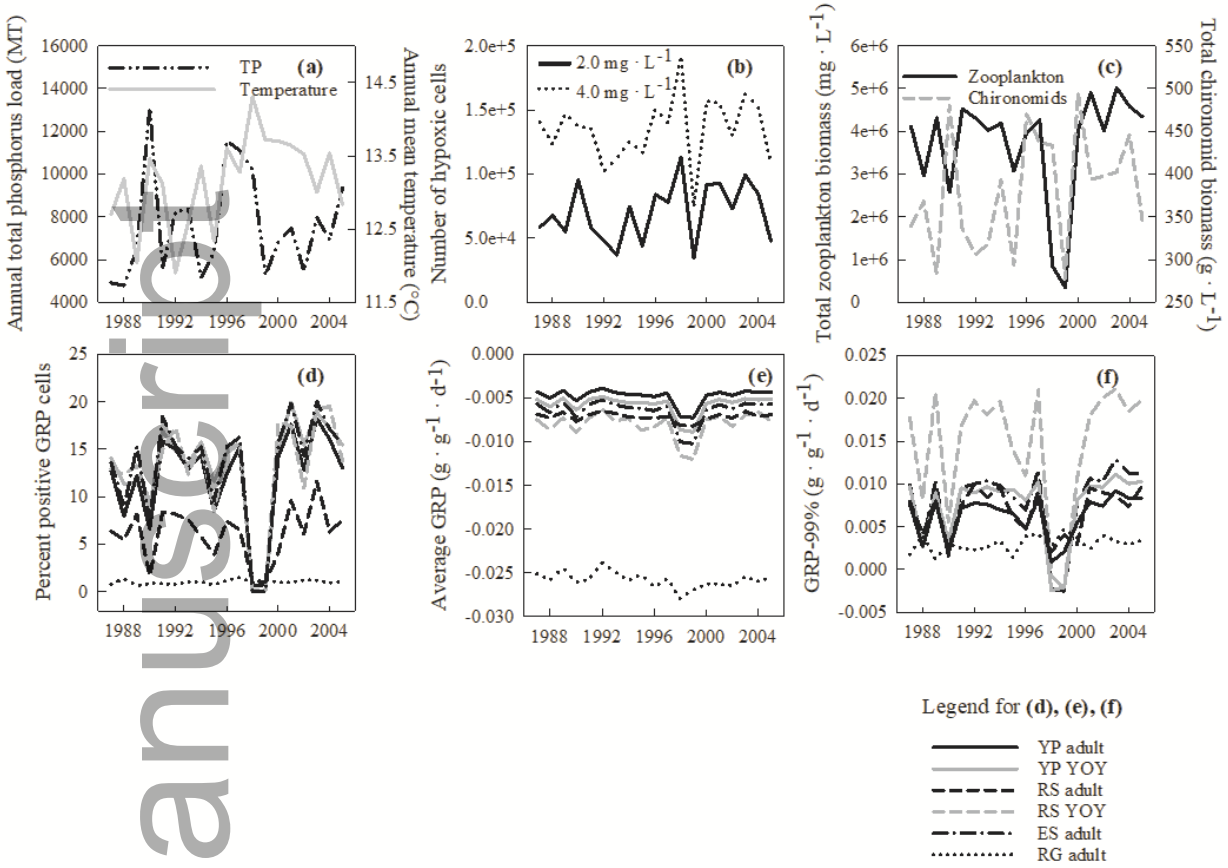

1044

1045

1046 Figure 4

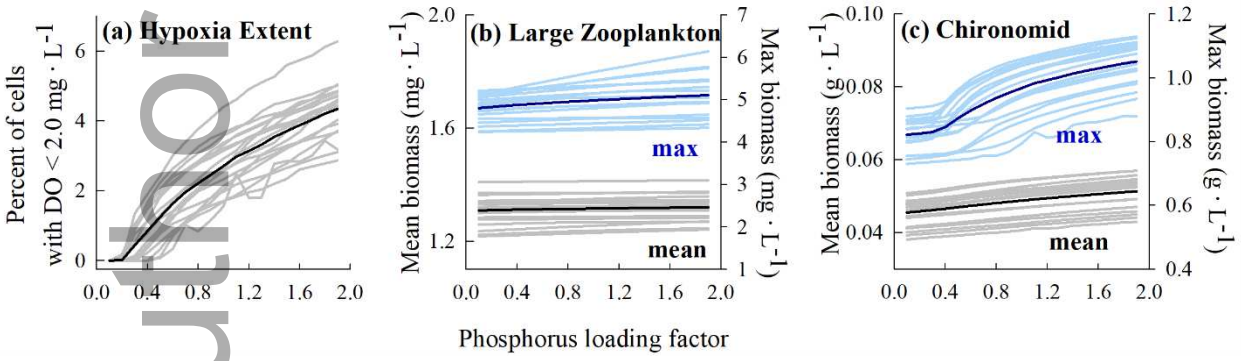

1047

1048

1049 Figure 5

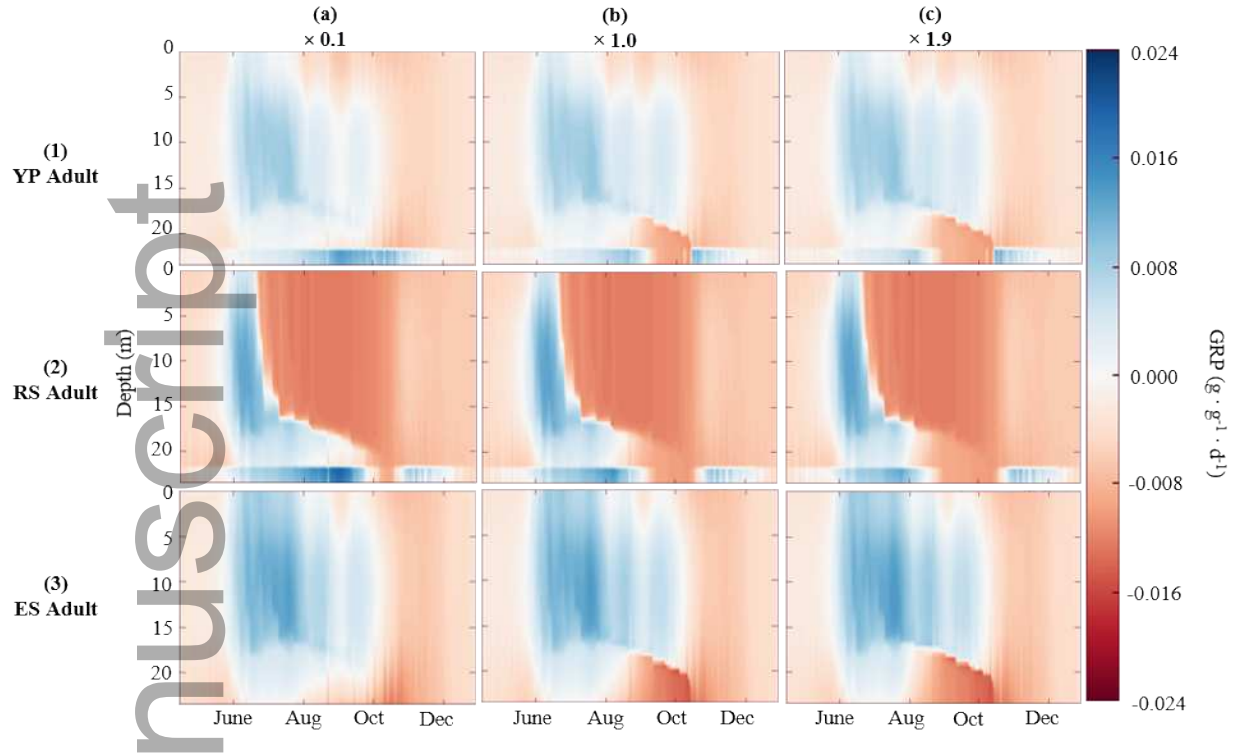

1050

1051

1052 Figure 6

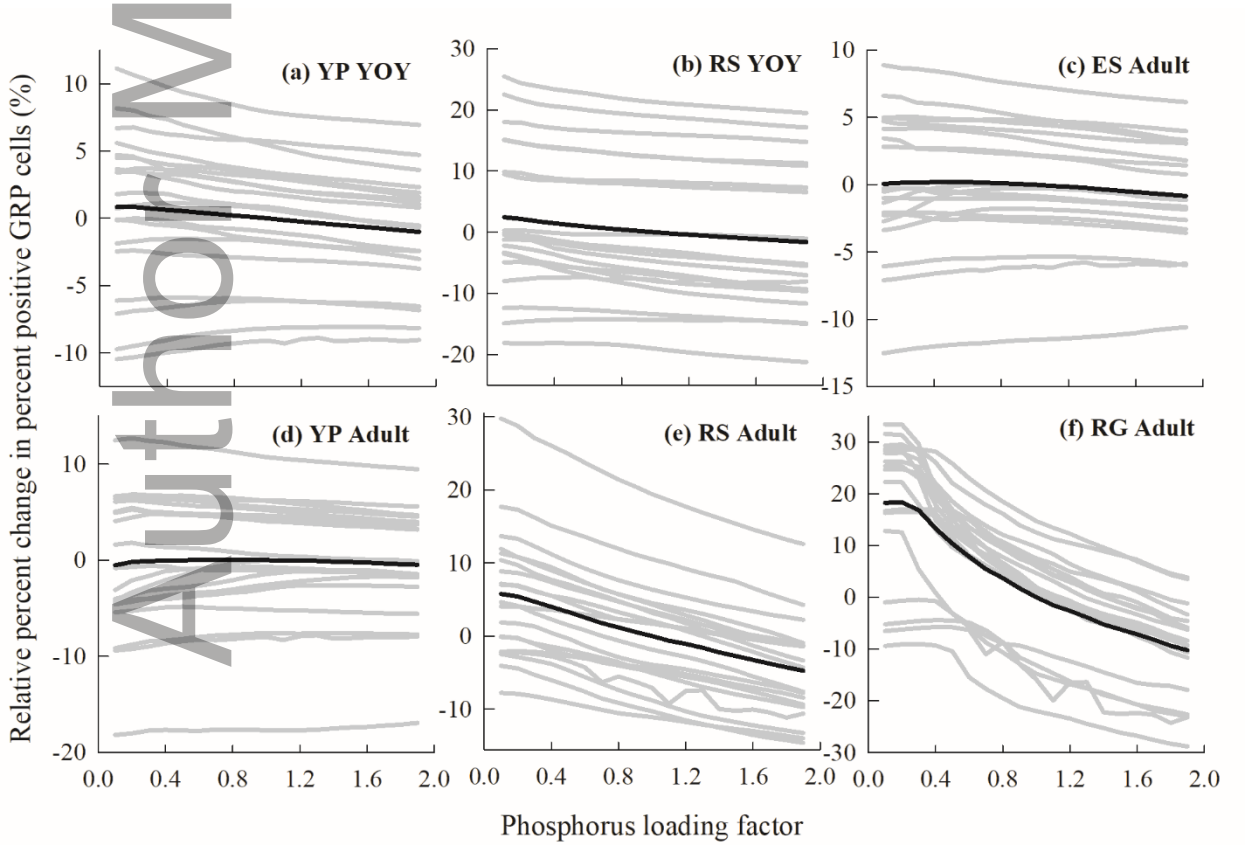

1053

1054

1055 Figure 7

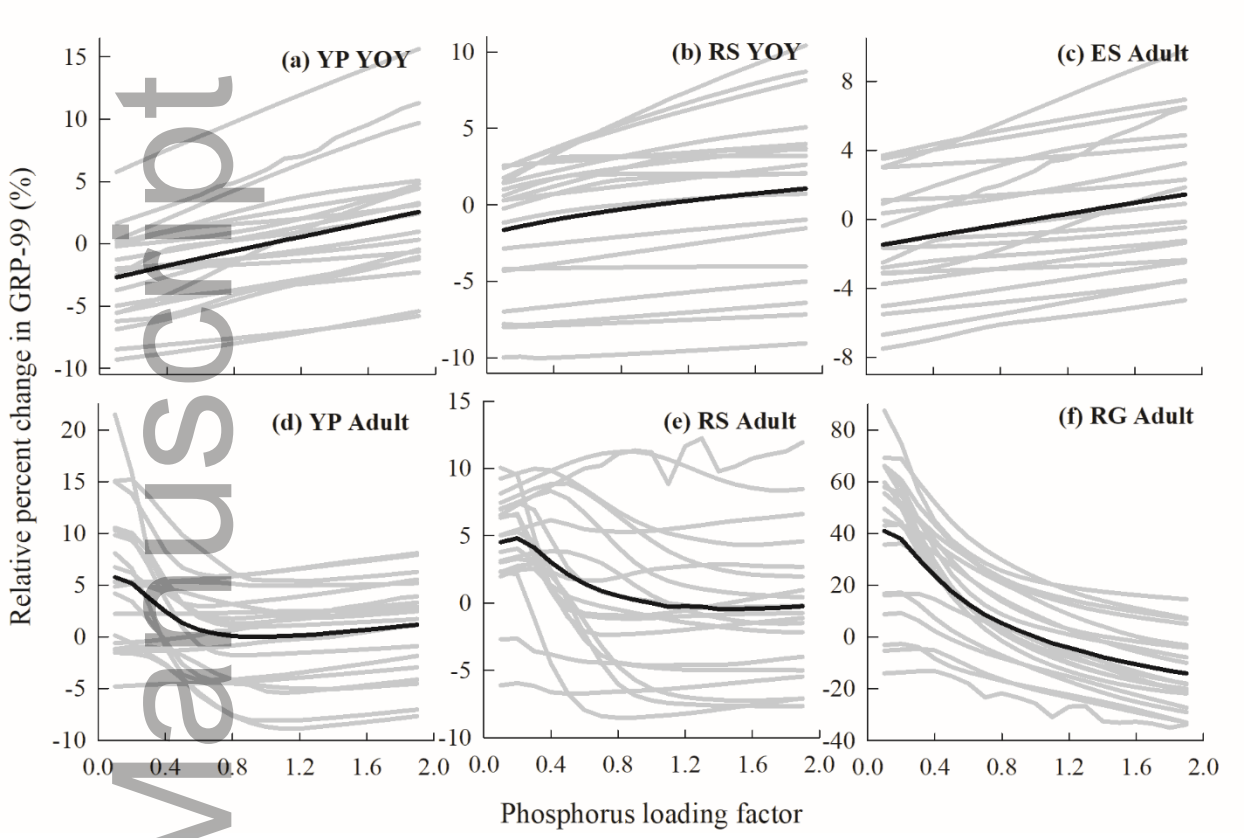

1056

1057

1058 Figure 8

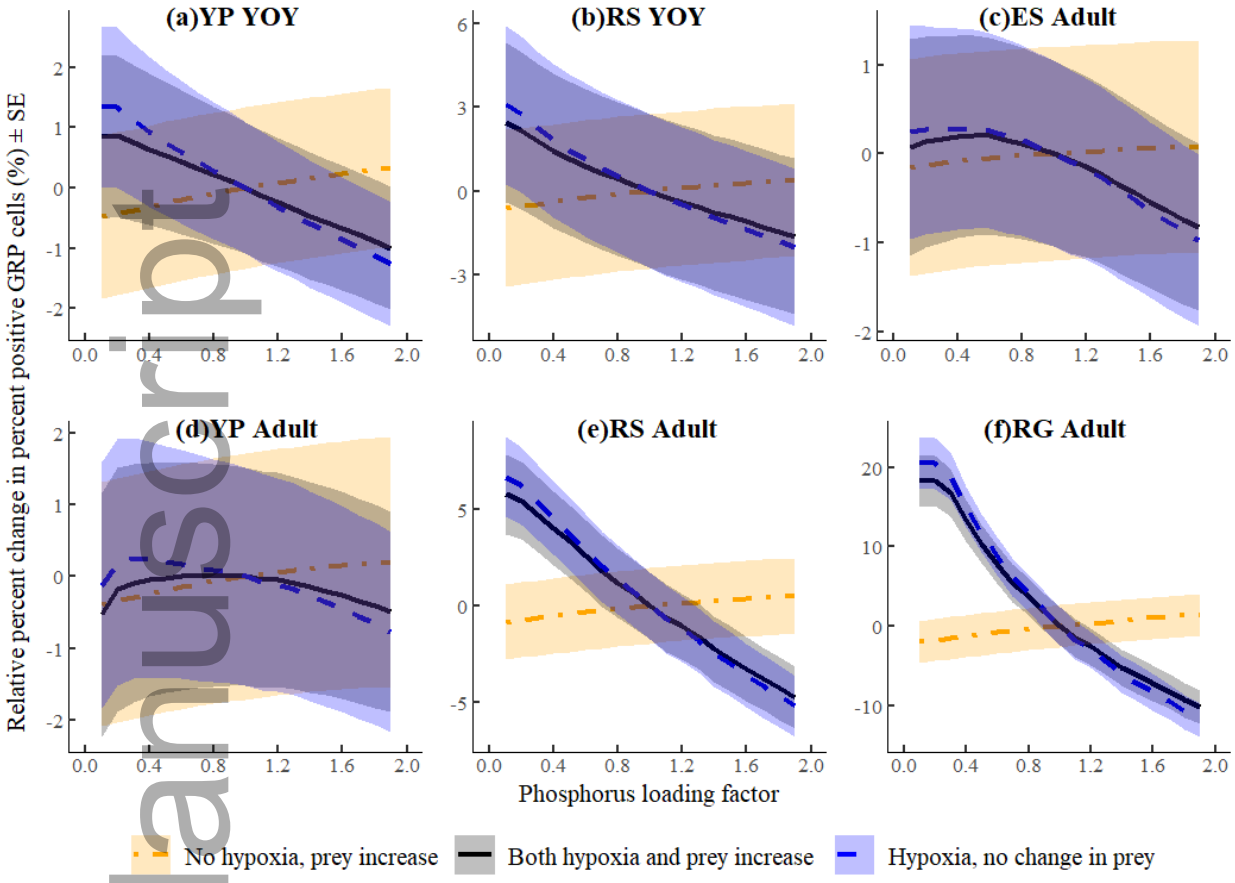

1059

Table 2: Spearman rank correlation coefficients (ρ) for relationships between pairs of annual values of biotic and abiotic habitat characteristics and two modeled habitat quality metrics (percent positive GRP and GRP-99%) in the hindcast simulation (n = 19 years). Biotic and abiotic habitat characteristics include total phosphorus (TP), temperature (°C, Temp), number hypoxia cells at ≤ 2.0 mg $\cdot$ L^{-1} (Hypoxia2), number of hypoxic cells at ≤ 4.0 mg $\cdot$ L^{-1} (Hypoxia4), total zooplankton biomass (mg $\cdot$ L^{-1}, ZP Bio), and total chironomid biomass (g $\cdot$ L^{-1}, Chiro Bio). Modeled habitat quality metrics include the annual growth rate potential (GRP) indices percent positive GRP (PP GRP) and GRP-99% for all species and life stages. The species codes are as follows: ES adult is adult emerald shiner, YP YOY is young-of-year yellow perch, RS YOY is young-of-year rainbow smelt, YP adult is adult yellow perch, RS adult is adult rainbow smelt, RG adult is adult round goby. Bolded values indicate strong correlations ($|\rho| \geq 0.80$) and underlined values indicate moderate to strong correlations ($|\rho| \geq 0.40$). * indicates that the correlation was significant ($P < 0.05$).

	TP	Temp	Hypoxia2	Hypoxia4	ZP Bio	Chiro Bio
TP						
Temp	0.10					
Hypoxia2	0.37	0.56*				
Hypoxia4	0.25	0.43	**0.85***			
ZP Bio	0.05	-0.32	0.13	0.26		
Chiro Bio	0.47*	0.59*	**0.85***	0.66*	0.01	
PP YP YOY	0.03	-0.05	0.24	0.23	**0.87***	0.23
PP YP adult	0.06	-0.14	0.21	0.24	**0.90***	0.19
PP RS YOY	0.11	-0.03	0.34	0.38	**0.81***	0.35
PP RS adult	0.17	-0.48*	-0.03	0.13	**0.85***	-0.16
PP ES adult	0.16	-0.12	0.25	0.37	**0.92***	0.23
PP RG adult	0.04	0.43	0.10	-0.12	-0.19	0.30
GRP99 YP YOY	0.10	-0.35	0.00	0.10	0.78*	0.03
GRP99 YP adult	0.10	-0.47*	-0.05	0.11	**0.86***	-0.09
GRP99 RS YOY	0.08	-0.51*	-0.05	0.03	0.72*	-0.08
GRP99 RS adult	-0.03	-0.48*	-0.24	-0.29	0.66*	-0.28

GRP99 ES adult	0.16	-0.40	0.04	0.16	**0.84***	0.02
GRP99 RG adult	0.03	0.53*	0.11	-0.14	-0.33	0.39

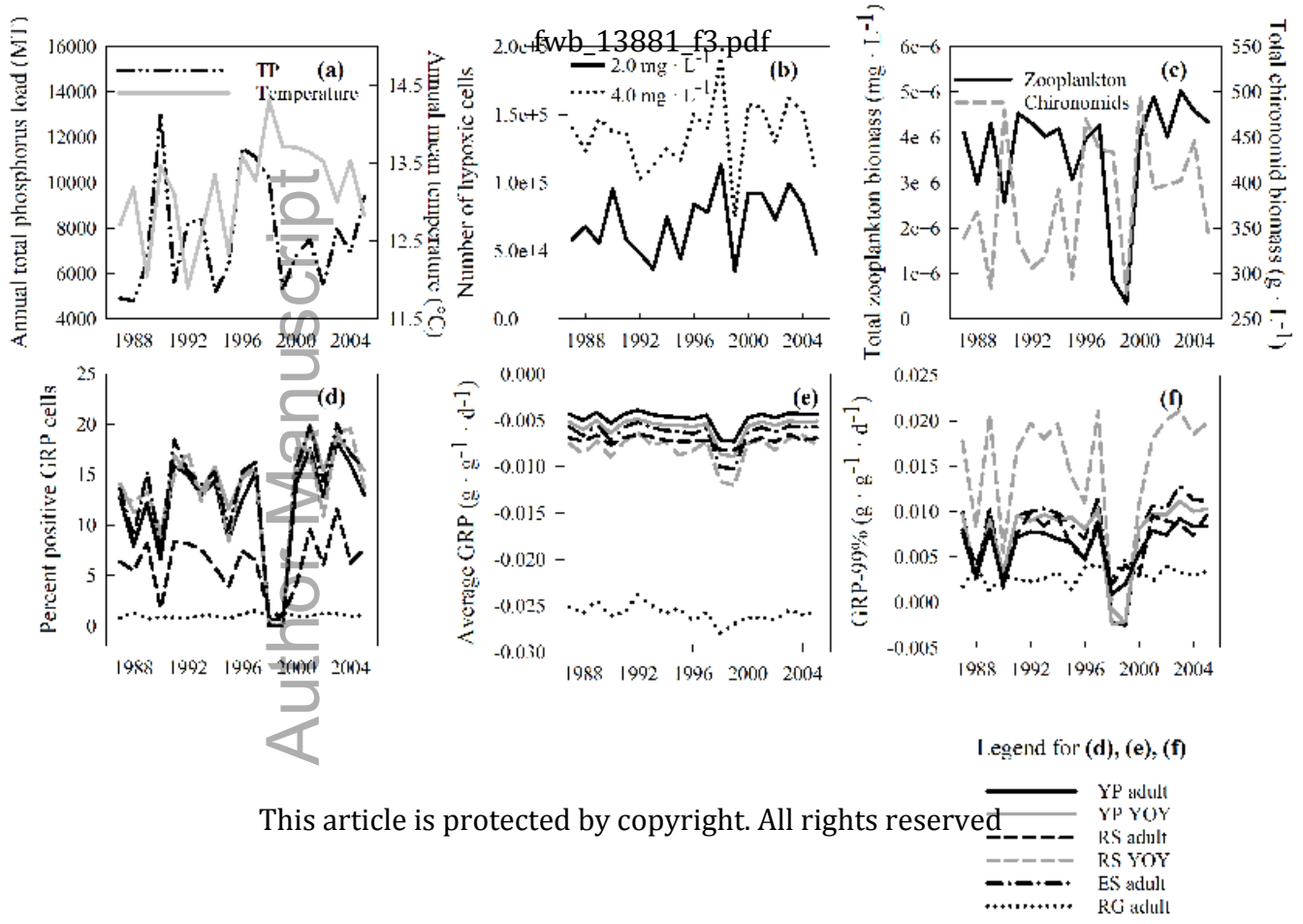

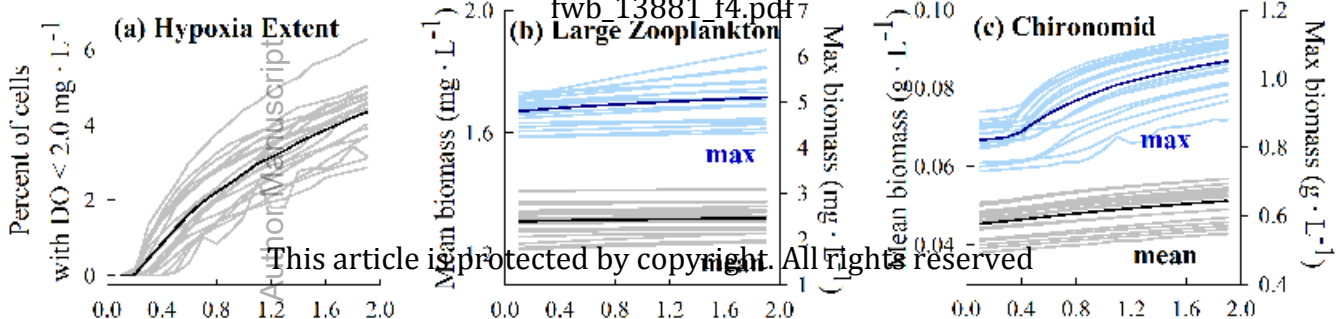

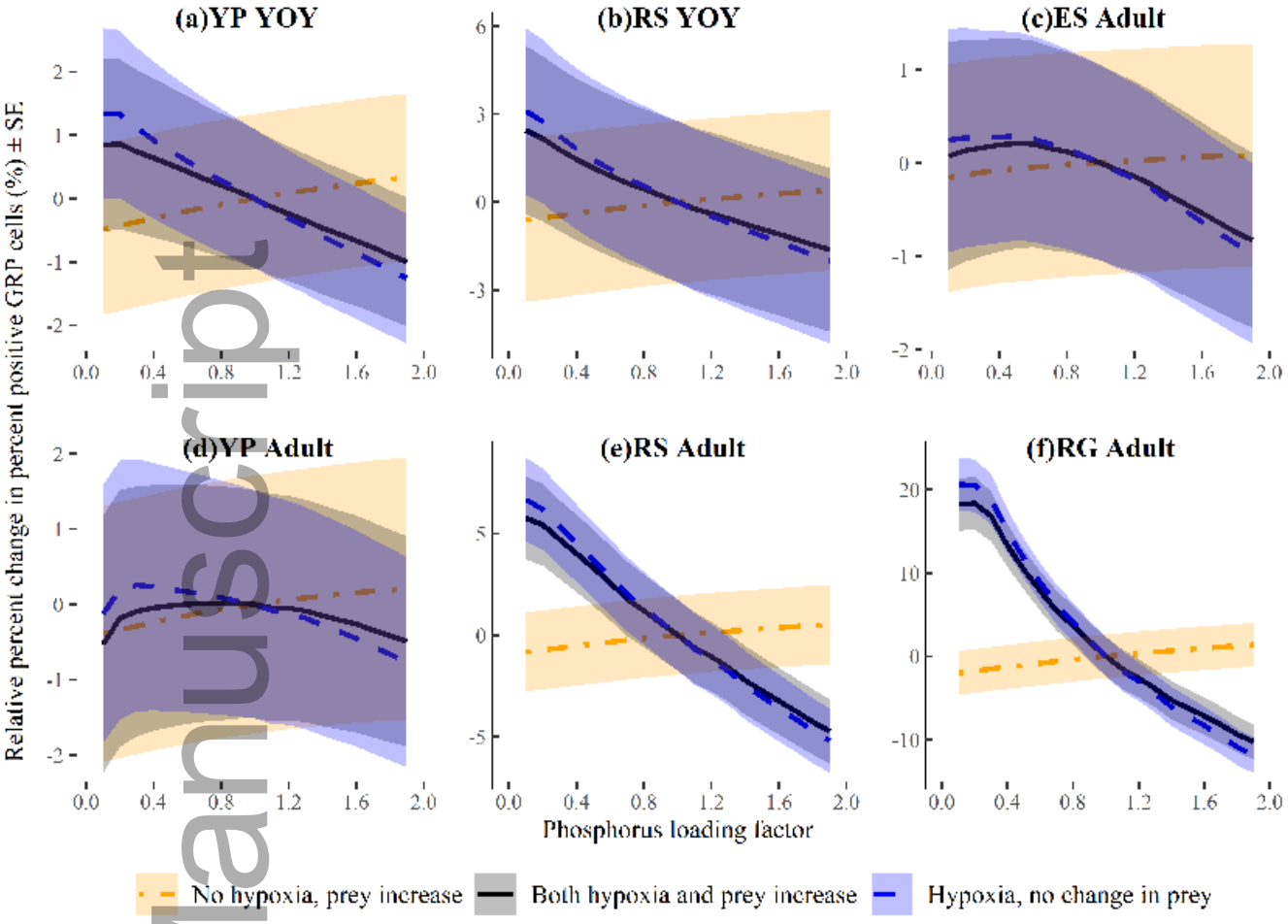

fwb_13881_f8.tif